

**REFERENCES**

1. Miller NR. Anatomy and Electrophysiology of the Retina. In: Miller NR, ed. *Walsh and Hoyt's Clinical Neuro-Ophthalmology*, Vol. 1, 4th edn. Baltimore: Williams & Wilkins, 1982; 41-59
2. Miller NR. Anatomy and Physiology of Optic Nerve. In: Miller NR, ed. *Walsh and Hoyt's Clinical Neuro-Ophthalmology*, Vol. 1, 4th edn. Baltimore: Williams & Wilkins, 1982; 41-59
3. Miller NR. Anatomy and Physiology of Optic Chiasm. In: Miller NR, ed. *Walsh and Hoyt's Clinical Neuro-Ophthalmology*, Vol. 1, 4th edn. Baltimore: Williams & Wilkins, 1982; 60-68
4. Miller NR. Anatomy and Physiology of Optic Tracts and Lateral Geniculate Body. In: Miller NR, ed. *Walsh and Hoyt's Clinical Neuro-Ophthalmology*, Vol. 1, 4th edn. Baltimore: Williams & Wilkins, 1982; 69-78
5. Miller NR. Anatomy and Physiology of Optic Radiations. In: Miller NR, ed. *Walsh and Hoyt's Clinical Neuro-Ophthalmology*, Vol. 1, 4th edn. Baltimore: Williams & Wilkins, 1982; 79-82
6. Miller NR. Anatomy and Physiology of Visual Cortex. In: Miller NR, ed. *Walsh and Hoyt's Clinical Neuro-Ophthalmology*, Vol. 1, 4th edn. Baltimore: Williams & Wilkins, 1982; 83-95
7. Rodiek RW, Binmoeller KF, Dineen J. Parasol and Midget Ganglion Cells of the Human Retina. *J Comp Neurol*. 1985; **233**: 115-32
8. Lee BB, Yeh T. Receptive fields of primate retinal ganglion cells studied with a novel technique. *Vis Neurosci*. 1998; **15**: 161-75
9. Schiller PH, Malpeli JG. Functional specificity of lateral geniculate nucleus . laminae of the rhesus monkey. *J Neurophysiol*. 1978; **41**: 788-97

10. Schiller PH, Logothetis NK, Charles ER. Functions of the colour-opponent and broad-band channels of the visual system. *Nature*. 1990; **343**: 68-70
11. Shapley R, Kaplan E, Soodak R. Spatial summation and contrast sensitivity of X and Y cells in the lateral geniculate nucleus of the macaque. *Nature*. 1981; **292**: 543-5
12. Casagrande VA, Ichida JM. The Lateral Geniculate Nucleus. In: Kaufman PL, Alm A, eds. *Adler's Physiology of the Eye*, 10th edn. St Louis: Mosby, 2003; chap 28
13. Dacey DM. Morphology of a small-field bistratified ganglion cell type in the macaque and human retina. *Vis Neurosci*. 1993; **10**: 1081-98
14. Livingstone M, Hubel D. Segregation of form, color, movement, and depth: anatomy, physiology, and perception. *Science*. 1988; **240**: 740-9
15. Dacey DM. Morphology of a small-field bistratified ganglion cell type in the macaque and human retina. *Vis Neurosci*. 1993; **10**: 1081-98
16. Kaplan E, Lee BB, Shapley RM. New views of primate retinal function. *Prog Retinal Res*. 1990; **9**: 273-336
17. Miller NR. Topical diagnosis of lesions in the visual sensory pathway. In: Miller NR, ed. *Walsh and Hoyt's Clinical Neuro-Ophthalmology*, Vol. 1, 4th edn. Baltimore: Williams & Wilkins, 1982; 108-52
18. McFadzem R, Brosnahan D, Hadley D, Mutlukan E. Representation of the visual field in the occipital striate cortex. *Br J Ophthalmol*. 1994; **78**: 185-90
19. Grochowicki M, Vighetto A. Homonymous horizontal sectoranopia: report of four cases. *Br J Ophthalmol*. 1991; **75**: 624-8
20. Johnson CA, Kelter JL. Automated suprathreshold status perimetry. *Am J Ophthalmol*. 1980; **89**: 731-41

21. Li SG, Spaeth GL, Scimeca HA, Schatz NJ, Savina PJ. Clinical experiences with the use of an automated perimeter (Octopus) in the diagnosis and management of patients with glaucoma and neurologic diseases. *Ophthalmology*. 1979; **86**: 1302–12
22. McCrary JA, Feigon J. Computerized perimetry in neuroophthalmology. *Ophthalmology*. 1979; **86**: 1287–301
23. Kramer SG. The peripheral visual field in glaucoma: Reevaluation in the age of automated perimetry. *Surv Ophthalmol*. 1991; **36**: 59–9
24. Kelter JL, Johnson CA, Spurr JO, Beck RW, Optic Neuritis Study Group. Baseline visual field profile of optic neuritis: the experience of the optic neuritis treatment trial. *Arch Ophthalmol*. 1993; **111**: 231–4
25. Goldberg I. Optic disc and visual field changes in primary open angle glaucoma. *Aust J Ophthalmol*. 1981; **9**: 223-9
26. Mitchell P, Smith W, Attebo K, Healey PR. Prevalence of open-angle glaucoma in Australia. The Blue Mountains Eye Study. *Ophthalmology*. 1996; **103**: 1661-9
27. Wensor MD, McCarty CA, Stanislavsky YL, Livingston PM, Taylor HR. The prevalence of glaucoma in the Melbourne Visual Impairment Project. *Ophthalmology*. 1998; **105**: 733-9
28. Morgan R.W, Drance S.M. Chronic Open Angle Glaucoma and Ocular Hypertension. An Epidemiological Study. *Br J Ophthalmol*. 1975; **59**: 211-5
29. Kronfeld PC. The history of glaucoma. In, Tasman W, Jaeger EA, eds. *Duane's Clinical Ophthalmology. revised ed.* Philadelphia: JB Lippincott 1993;3.chap.41
30. Douglas GR. Pathogenetic mechanisms of glaucoma not related to intraocular pressure. *Curr Opin Ophthalmol*. 1998; **9**: 34-8

31. Yamamoto T, Kitazawa Y. Vascular pathogenesis of normal-tension glaucoma: a possible pathogenetic factor, other than intraocular pressure, of glaucomatous optic neuropathy. *Prog Retinal Eye Res.* 1998; **17**: 127-43
32. WuDunn D. Genetic basis of glaucoma. *Curr Opin Ophthalmol.* 2002; **13**: 55-60
33. Uhm K-B, Shin D.H. Positive Family History of Glaucoma is a Risk Factor for Increased IOP rather than Glaucomatous Optic Nerve Damage (POAG vs OH vs Normal Control). *Korean J Ophthalmol.* 1992; **6**: 100-4
34. Orgül S, Flammer J. Headache in Normal Tension Glaucoma Patients. *J Glaucoma.* 1994; **3**: 292-5
35. Graham S. Are Vascular Factors Involved in Glaucomatous Damage? *Aust NZ J Ophthalmol.* 1999; **27**: 354-7
36. Flammer J. The Vascular Concept of Glaucoma. *Surv Ophthalmol.* 1994; **38**: S3-S6
37. Gasser P, Flammer J. Blood-cell Velocity in the Nailfold Capillaries of Patients with Normal Tension and High Tension Glaucoma. *Am J Ophthalmol.* 1991; **111**: 585-8
38. Gasser P, Flammer J, Gauthauser U et al. Do Vasospasms Provoke Ocular Diseases? *Angiology.* 1990; **Mar**: 213-20
39. Gasser P, Flammer P. Short- and Long-Term Effects of Nifedipine on the Visual Field in Patients with Presumed Vasospasm. *J Int Med Res.* 1990; **18**: 334-9
40. Ritch R. Order in Glaucoma. *Int Glaucoma Rev.* 1999; **1-3**: 13
41. Quigley H.A, Enger L, Katz J et al. Risk Factors for the Development of Glaucomatous Visual Field Loss in Ocular Hypertension. *Arch Ophthalmol.* 1994; **112**: 644-9

42. Sommer A, Tielsch J.M, Katz J *et al.* Relationship Between Intraocular Pressure and Primary Open Angle Glaucoma Among White and Black Americans. *Arch Ophthalmol.* 1991; **109**: 1090-5
43. Kass MA, Heuer DK, Higginbotham EJ *et al.* The Ocular Hypertensive Treatment Study: A Randomized Trial Determines that Topical Ocular Hypotensive Medication Delay or Prevents the Onset of Primary Open-Angle Glaucoma. *Arch Ophthalmol.* 2002; **120**: 701-13
44. Heijl A, Leske C, Bengtsson B *et al.* Reduction of Intraocular Pressure and Glaucoma Progression: Results from the Early Manifest Glaucoma Trial. *Arch Ophthalmol.* 2002; **120**: 1268-79
45. Collaborative Normal-Tension Glaucoma Study Group. The Effectiveness of Intraocular Pressure Reduction in the Treatment of Normal-Tension Glaucoma. *Am J Ophthalmol.* 1998; **126**: 498-505
46. The Advanced Glaucoma Intervention Study (AGIS): 7. The Relationship between control of intraocular pressure and visual field deterioration. The AGIS Investigators. *Am J Ophthalmol.* 2000; **130**: 429-40
47. Phelps C.D. Glaucoma. General Concepts. In: Tasman W, Jaeger E.A., eds. *Duane's Clinical Ophthalmology.* revised ed. Philadelphia: JB Lippincott, 1993; Vol. 3, Chap. 42: 1-2
48. Hart W.M, Becker B. The Onset and Evolution of Glaucomatous Visual Field Defects. *Ophthalmology.* 1982; **89**: 268-79
49. Tuck M, Crick R.P. The Age Distribution of Primary Open Angle Glaucoma. *Oph Epidemiol.* 1998; **5**: 173-83
50. Georgopoulos G, Andeanos D, Liokis N *et al.* Risk Factors in Ocular Hypertension. *Eur J Ophthalmol.* 1997; **7**: 357-63

51. Uhm K-B, Shin D.H. Glaucoma Risk Factors in Primary Open Angle Glaucoma Patients Compared to Ocular Hypertensives and Control Subjects. *Korean J Ophthalmol.* 1992; **6**: 91-9
52. Wienreb R. Why Study the Ocular Microcirculation in Glaucoma. *J Glaucoma.* 1992; **1**: 145-7
53. Mitchell P, Smith W, Chey T et al. Open Angle Glaucoma and Diabetes. *Ophthalmology.* 1997; **104**: 712-8
54. Leighton D.A, Phillips C.I. Systemic Blood Pressure in Open Angle Glaucoma, Low Tension Glaucoma and the Normal Eye. *Br J Ophthalmol.* 1972; **56**: 447-53
55. Zeiter J.H, Shin D.H, Baek N.H. Visual Field Defects in Diabetic Patients with Primary Open Angle Glaucoma. *Am J Ophthalmol.* 1991; **111**: 581-4
56. McLeod S.D, West S.K, Quigley H.A et al. A Longitudinal Study of the Relationship Between Intraocular and Blood Pressures. *Invest Ophthalmol Vis Sci.* 1990; **31**: 2361-6
57. Wilson M.R, Hertzmark E, Walker A.M et al. A Case-Control Study of Risk Factors in Open Angle Glaucoma. *Arch Ophthalmol.* 1987; **105**: 1066-71
58. Klein B.E.K, Klein R, Moss S.E. Incidence of Self Reported Glaucoma in People with Diabetes Mellitus. *Br J Ophthalmol.* 1997; **81**: 743-7
59. Schwartz B, Tomita G, Takamoto T. Glaucoma-Like Discs with Subsequent Increased Ocular Pressures. *Ophthalmology.* 1991; **98**: 41-9
60. Wang J.J, Mitchell P, Smith W. Is There An Association Between Migraine Headache and Open Angle Glaucoma. *Ophthalmology.* 1997; **104**: 1714-9
61. Phelps C.D, Corbett J.J. Migraine and Low Tension Glaucoma. *Invest. Ophthalmol Vis Sci.* 1985; **26**: 1105-8

62. Drance S.M, Douglas G.R, Wijsman K *et al.* Response of Blood Flow to Warm and Cold in Normal and Low Tension Glaucoma Patients. *Am J Ophthalmol.* 1988; **105**: 35-9
63. Guthauser U, Flammer J, Mahler F. The Relationship Between Digital and Ocular Vasospasm. *Graefe's Arch Clin Exp Ophthalmol.* 1988; **226**: 224-6
64. Gasser P, Flammer J. Influence of Vasospasm on Visual Function. *Doc Ophthalmol.* 1987; **66**: 3-18
65. Chai E, Goldberg I, Chia A *et al.* Visual Field Responses to a Hand Vibration Stimulus. *Surv Ophthalmol.* 1999; **43 [Suppl 1]**: S79-S86
66. Hayreh S.S. Interindividual Variation in Blood Supply of the Optic Nerve Head. *Doc Ophthalmol.* 1985; **59**: 217-46
67. Leske M.C, Connell A.M.S, Wu S.Y *et al.* Risk Factors for Open Angle Glaucoma. The Barbados Eye Study. *Arch Ophthalmol.* 1995; **113**: 918-24
68. Rosenthal R, Perkins E.S. Family Studies in Glaucoma. *Br J Ophthalmol.* 1985; **69**: 664-7
69. Tielsch J.M, Katz J, Sommer A *et al.* Family History and Risk of Primary Open Angle Glaucoma. *Arch Ophthalmol.* 1994; **112**: 69-72
70. Stone EM, Fingert JH, Alward WLM, Nguyen TD, Polansky JR, Sunden SLF *et al.* Identification of a gene that causes primary open angle glaucoma. *Science.* 1997; **275**: 668-70
71. Sheffield VC, Stone EM, Alward WL, Drack AV, Johnson AT, Streb LM, Nichols BE. Genetic linkage of familial open angle glaucoma to chromosome 1q21-q31. *Nat Genet.* 1993; **4**: 47-50
72. Kubota R, Noda S, Wang Y, Minoshima S, Asakawa S, Kudoh J *et al.* A novel myosin-like protein (myocilin) expressed in the connecting cilium of the

- photoreceptor: molecular cloning, tissue expression, and chromosomal mapping. *Genomics*. 1997; **41**: 360-9
73. Sarfarazi M, Child A, Stoilova D, Brice G, Desai T, Trifan OC *et al.* Localization of the fourth locus (GLC1E) for adult onset primary open angle glaucoma to the 10p15-p14 Region. *Am J Hum Genet*. 1998; **62**: 641-52
74. Stoilova D, Child A, Trifan OC, Crick RP, Coakes RL, Sarfarazi M. Localization of a locus (GLC1B) for adult-onset primary open angle glaucoma to the 2cen-q13 region. *Genomics*. 1996; **36**: 142-50
75. Wirtz MK, Samples JR, Kramer PL, Rust K, Topinka JR, Yount J *et al.* Mapping a gene for adult-onset primary open-angle glaucoma to chromosome 3q. *Am J Hum Genet*. 1997; **60**: 296-304
76. Trifan OC, Traboulsi EI, Stoilova D, Alozie I, Nguyen R, Raja S, Sarfarazi M. A third locus (GLC1D) for adult-onset primary open-angle glaucoma maps to the 8q23 region. *Am J Ophthalmol*. 1998; **126**: 17-28
77. Wirtz MK, Samples JR, Rust K, Lie J, Nordling L, Schilling K, Acott TS, Kramer PL. GLC1F, a new primary open-angle glaucoma locus, maps to 7q35-q36. *Arch Ophthalmol*. 1999; **117**: 237-41
78. Faucher M. Anctil JL. Rodrigue MA. Duchesne A. Bergeron D. Blondeau P. Cote G. Dubois S. Bergeron J. Arseneault R. Morissette J. Raymond V. Quebec Glaucoma Network. Founder TIGR/myocilin mutations for glaucoma in the Quebec population. *Hum Mol Genet*. 2002; **11**: 2077-90
79. Alward WL *et al.* Clinical features associated with mutations in the chromosome1 open-angle glaucoma gene (GLC1A). *N Engl J Med*. 1998; **338**: 1022-7
80. Wiggs JL *et al.* Prevalence of mutations in TIGR/myocilin in patients with adult and juvenile primary open-angle glaucoma. *Am J Hum Genet*. 1998; **63**: 1549-52



81. Challa P *et al.* Prevalence of myocilin mutations in adults with primary open angle glaucoma in Ghana, West Africa. *J Glaucoma*. 2002; **11**: 416–20
82. Rezaie T *et al.* Adult-onset primary open-angle glaucoma caused by mutations in optineurin. *Science*. 2002; **295**: 1077–9
83. Mitchell P, Hourihan F, Sandbach J *et al.* The Relationship Between Glaucoma and Myopia. *Ophthalmology*. 1999; **106**: 2010-5
84. Nickells RW. Retinal ganglion cell death in glaucoma: the how, the why, and the maybe. *J Glaucoma*. 1996; **5**: 345-56
85. Spaeth GL. Glaucoma, apoptosis, death, and life. *Acta Ophthalmol Scand Suppl*. 1998; **227**: 9-15
86. Garcia-Valenzuela E, Shareef S, Walsh J *et al.* Programmed cell death of retinal ganglion cells during experimental glaucoma. *Exp Eye Res*. 1995; **61**: 33-44
87. Quigley HA, Nickells RW, Kerrigan LA, Pease ME, Thibault DJ, Zack DJ. Retinal ganglion cell death in experimental glaucoma and after axotomy occurs by apoptosis. *Invest Ophthalmol Vis Sci*. 1995; **36**: 774-86
88. Lipton SA, Rosenberg PA. Excitatory amino acids as a final common pathway for neurologic disorders. *N Engl J Med*. 1994; **330**: 613-622
89. Oppenheim RW. Cell death during development of the nervous system. *Ann Rev Neurosci*. 1991; **14**: 453-501
90. Pease ME, McKinnon SJ, Kerrigab-Baumrind LA, Zack DJ. Obstructed axonal transport of BDNF and its receptor TrkB in experimental glaucoma. *Invest Ophthalmol Vis Sci*. 2000; **41**: 764-74
91. Anderson DR, Hendrickson A. Effect of intraocular pressure on rapid axoplasmic transport in monkey optic nerve. *Invest Ophthalmol Vis Sci*. 1974; **13**: 771-83

92. Radius RL, Anderson DR. Rapid axonal transport in primate optic nerve. *Arch Ophthalmol*. 1981; **99**: 650-4
93. Dreyer EB. A proposed role for excitotoxicity in glaucoma. *J Glaucoma*. 1998; **7**: 62-7
94. Vorwerk CK, Gorla MS, Dreyer EB. An experimental basis for implicating excitotoxicity in glaucomatous optic neuropathy. *Surv Ophthalmol*. 1999; **43 [Suppl 1]**: S142-50
95. Neufeld AH. Nitric oxide: a potential mediator of retinal ganglion cell damage in glaucoma. *Surv Ophthalmol*. 1999; **43 [Suppl 1]**: S129-35
96. Choi DW. Glutamate neurotoxicity and diseases of the nervous system. *Neuron*. 1988; **1**: 623-634
97. Vorwerk CK, Hyman BT, Miller JW, Husain D, Zurakowski D, Huang PL, Fishman MC, Dreyer EB. The role of neuronal and endothelial nitric oxide synthase in retinal excitotoxicity. *Invest Ophthalmol Vis Sci*. 1997; **38**: 2038-44
98. Brune B, von Knethen A, Sandau KB. Nitric oxide and its role in apoptosis. *Eur J Pharmacol*. 1998; **35**: 261-72
99. Brune B, Sandau KB, von Knethen A. Apoptotic cell death and nitric oxide: activating and antagonistic transducing pathways. *Biochemistry*. 1998; **63**: 817-25
100. Roth S. Role of nitric oxide in retinal cell death. *Clin Neurosci*. 1997; **4**: 216-23
101. Naskar R, Dreyer EB. New horizons in neuroprotection. *Surv Ophthalmol*. 2001; **45 [Suppl 3]**: S250-5
102. Morgan J, Caprioli J, Koseki Y. Nitric oxide mediates excitotoxic and anoxic damage in rat retinal ganglion cells cocultured with astroglia. *Arch Ophthalmol*. 1999; **117**: 1524-9

103. Neufeld AH, Hernandez MR, Gonzalez M. Nitric oxide synthase in the human glaucomatous optic nerve head. *Arch Ophthalmol.* 1997; **115**: 497-503
104. Hitchings RA, Spaeth GL. The optic disc in glaucoma. I. Classification. *Br J Ophthalmol.* 1976; **60**: 778-5
105. Hitchings RA, Spaeth GL. The optic disc in glaucoma. II. Correlation of the appearance of the optic disc with visual field. *Br J Ophthalmol.* 1977; **61**: 107-13
106. Yamagishi N, Anton A, Sample P, Zangwill L, Lopez A, Weinreb R. Mapping structural damage of the optic disk to visual field defect in glaucoma. *Am J Ophthalmol.* 1997; **123**: 667-76
107. Broadway DC, Nicoletta MT, Drance SM. Optic disk appearances in primary open-angle glaucoma. *Surv Ophthalmol.* 1999; **43 [Suppl 1]**: S223-43
108. Young H, Kwon, Chang-sik Kim, M. Bridget Zimmerman, Wallace L. M. Alward and Sohan S. Hayreh. Rate of visual field loss and long-term visual outcome in primary open-angle glaucoma. *Am J Ophthalmol.* 2001; **132**: 47-56
109. Lichter PR. Glaucoma clinical trials and what they mean for our patients. *Am J Ophthalmol.* 2003; **136**: 136-45
110. Heijl A, Lundqvist L. The frequency distribution of earliest glaucomatous visual field defects documented by automated perimetry. *Acta Ophthalmol.* 1984; **62**: 658-64
111. Kitazawa Y, Takahashi O, Ohiwa Y. The mode of development and progression of field defects in early glaucoma - a follow up study. *Doc Ophthalmol Proc Ser.* 1980; **19**: 211-20
112. Kendell KR, Quigley HA, Kerrigan LA, Pease ME, Quigley EN. Primary open-angle glaucoma is not associated with photoreceptor loss. *Invest Ophthalmol Vis Sci.* 1995; **36**: 200-5

113. Eagle RC ed. *Eye Pathology: An Atlas and Basic Text*. Philadelphia: W.B Saunders, 1999; chap 7
114. Levin LA. Relevance of the site of injury of glaucoma to neuroprotective strategies. *Surv Ophthalmol*. 2001; **45**[Suppl 3]: S243-S249
115. Chen PP. Risk and risk factors for blindness from glaucoma. *Curr Opin Ophthalmol*. 2004; **15**: 107-11
116. Chen PP. Blindness in patients with treated open-angle glaucoma. *Ophthalmology*. 2003; **110**: 726-33
117. Grant WM, Burke JF Jr. Why do some people go blind from glaucoma?. *Ophthalmology*. 1982; **89**: 991-8
118. Wolfs RCW, Borger PH, Ramrattan RS *et al*. Changing views on open-angle glaucoma: definition and prevalence. The Rotterdam Study. *Invest. Ophthalmol. Vis. Sci*. 2000; **41**: 3309–21
119. Von Graefe A. Ueber die Untersuchung des Gesichtsfeldes bei amblyopischen Affektionen. *Von Graefe's Arch Ophthalmol*. 1856; **2**: 258-98
120. Bjerrum BJ. An addition to the usual visual field examination and the visual field in glaucoma. *Nordisk Oftalmologisk Tidsskrift* 1889; **2**: 141–85
121. Aubert H, Förster R. Beiträge zur Kenntniss des indirecten Sehens. Untersuchungen über den Raumsinn der Retina. *Von Graefe's Arch Ophthalmol*. 1857; **3**: 1-37
122. Traquair HM. Perimetry in the study of glaucoma. *Trans Ophthalmol UK*. 1931; **51**: 585-99
123. Goldmann H. Ein selbstregistrierendes Projektionskugelperimeter. *Ophthalmologica*. 1945; **109**: 71-9

124. Beck RW, Berstrom TJ, Lichter PR. A clinical comparison of visual field testing with a new automated perimeter, the Humphrey Field Analyzer, and the Goldmann Perimeter. *Ophthalmology* 1985; **92**: 77–82
125. Katz J, Sommer A. Asymmetry and variation in the normal hill of vision. *Arch Ophthalmol* 1986; **104**: 65-68
126. Stewart WC, Shields MB. The peripheral visual field in glaucoma: reevaluation in the age of automated perimetry. *Surv Ophthalmol.* 1991; **36**: 59-69
127. Harrington D. *The Visual Fields*. 4<sup>th</sup> Ed. St Louis, CV Mosby Co. 1976, p 14-24
128. Frankhauser F, Spahr J, Bebie H. Some aspects of the automation of perimetry. *Surv Ophthalmol.* 1977; **22**: 131-41
129. Trobe JD, Acosta PC, Shuster JJ, Krischer JP. An evaluation of the accuracy of community-based perimetry. *Am J Ophthalmol.* 1980; **90**: 654-60
130. Portney GL, Krohn MA. Automated Perimetry: Background, Instruments and Methods. *Surv Ophthalmol.* 1978; **22**: 271-8
131. Johnson CA. Role of automation in new instrumentation. *Optom Vis Sci* 1993; **70**: 288–98
132. Katz J, Quigley HA, Sommer A. Repeatability of the glaucoma Hemifield test in automated perimetry. *Invest Ophthalmol Vis Sci.*; 1995; **36**: 1658–64
133. Heijl A. Automatic Perimetry in Glaucoma Visual Screening; A Clinical Study. *Graefes Arch Clin Exp Ophthalmol.* 1976; **200**: 21-37
134. Johnson CA, Keltner JL. Automated Suprathreshold Static Perimetry. *Am J Ophthalmol.* 1980; **89**: 731-41
135. Li SG, Spaeth GL, Scimeca HA et al. Clinical Experiences with the Use of An Automated Perimeter (Octopus) in the Diagnosis and Management of Patients with Glaucoma and Neurologic Diseases. *Ophthalmology.* 1979; **86**: 1302-12

136. Parr JC. To lessen the tedium of perimetry. *Trans Ophthalmol Soc NZ*. 1984; **36**: 16-22
137. McCrary JA, Feigon J. Computerized perimetry in neuroophthalmology. *Ophthalmology* 1979; **86**: 1287–301
138. Bengtsson B, Olsson J, Heijl A, Rootzen H. A new generation of algorithms for computerized threshold perimetry, SITA. *Acta Ophthalmol Scand*. 1997; **75**: 368-75
139. Flanagan JG, Wild JM, Trope GE. Evaluation of FASTPAC, a new strategy for threshold estimation with the Humphrey Field Analyzer, in a glaucomatous population. *Ophthalmology*. 1993; **100**: 949-54
140. Sharma AK, Goldberg I, Graham SL, et al. Comparison of the Humphrey Swedish Interactive Thresholding Algorithm (SITA) and full threshold strategies. *J Glaucoma* 2000; **9**: 20–7
141. Bengtsson B, Olsson J, Heijl A, et al. A new generation of algorithms for computerised threshold perimetry, SITA. *Acta Ophthalmol (Scand)*. 1997; **75**: 368–75
142. Flammer J. The concept of visual field indices. *Graefes Arch Clin Exp Ophthalmol*. 1986; **224**: 389-92
143. Flammer J, Drance SM, Augustiny L, Funkhouser A. Quantification of glaucomatous visual field defects with automated perimetry. *Invest Ophthalmol Vis Sci*. 1985; **26**: 176-81
144. Pearson PA, Baldwin LB, Smith TJ. The relationship of mean defect to corrected loss variance in glaucoma and ocular hypertension. *Ophthalmologica*. 1990; **200**: 16-21

145. Kook MS, Yang SJ, Kim S, Chung J, Kim ST, Tchah H. Effect of cataract extraction on frequency doubling technology perimetry. *Am J Ophthalmol.* 2004; **138**: 85-90
146. Gordon MO, Beiser JA, Brandt JD *et al.* The Ocular Hypertensive Treatment Study: Baseline Factors that Predict the Onset of Primary Open-Angle Glaucoma. *Arch Ophthalmol.* 2002; **120**: 714-20
147. Asman P, Heijl A. Evaluation of methods for automated Hemifield analysis in perimetry. *Arch Ophthalmol* 1992; **110**: 820-6
148. Asman P, Heijl A. Glaucoma Hemifield Test. Automated visual field evaluation. *Arch Ophthalmol.* 1992; **110**: 812-9
149. Heijl A, Krakau CE. An automatic static perimeter, design and pilot study. *Acta Ophthalmologica (Copenh).* 1975; **53**: 293-310
150. Katz J, Sommer A. Reliability Indices of Automated Perimetric Tests. *Arch Ophthalmol.* 1998; **106**: 1252-4
151. Koucheiki B, Nouri-Mahdavi K, Patel G, Gaasterland D, Caprioli J. Visual field changes after cataract extraction: the AGIS experience. *Am J Ophthalmol.* 2004; **138**: 1022-8
152. Quigley HA. Early detection of glaucomatous damage. Changes in the appearance of the optic disc. *Surv. Ophthalmol.* 1985; **30**: 111-26
153. Zeyen TG, Caprioli J. Progression of disc and field damage in early glaucoma. *Arch Ophthalmol.* 1993; **111**: 62-5
154. Johnson CA, Sample PA, Zangwill LM, Vasile CG, Cioffi GA, Liebmann JR, Weinreb RN. Structure and function evaluation (SAFE): II. Comparison of optic disk and visual field characteristics. *Am J Ophthalmol.* 2003; **135**: 148-54
155. Quigley HA, Addicks EM, Green R. Optic nerve damage in human glaucoma. *Arch. Ophthalmol.* 1982; **100**: 135-46

156. Harwerth RS, Carter-Dawson L, Shen F, Smith EL, Crawford MLJ. Ganglion cell losses underlying visual field defects from experimental glaucoma. *Invest Ophthalmol Vis Sci.* 1999; **40**: 2242-50
157. Johnson CA. Early losses of visual function in glaucoma. *Optom Vis Sci.* 1995; **72**: 359-70
158. Quigley HA, Sanchez RM, Dunkelberger GR, L'Hernault NL, Baginski TA. Chronic glaucoma selectively damages large optic nerve fibres. *Invest Ophthalmol Vis Sci.* 1987; **28**: 913-20
159. Glovinsky Y, Quigley HA, Dunkelberger GR. RGC loss is size dependent in experimental glaucoma. *Invest Ophthalmol Vis Sci.* 1991; **32**: 484-91
160. Quigley HA, Dunkelberger GR, Green WR. Chronic human glaucoma causing selectively greater loss of large optic nerve fibres. *Ophthalmology* 1988; **95**: 357-63
161. Quigley HA, Green WR. The histology of human glaucoma cupping and optic nerve damage: clinicopathologic correlation in 21 eyes. *Ophthalmology* 1979; **86**: 1803-27
162. Radius R, Gonzales M. Anatomy of the lamina cribrosa in human eyes. *Arch Ophthalmol.* 1981; **99**: 2159-62
163. Sanchez RM, Dunkelberger GR, Quigley HA. The number and diameter distribution of axons in the monkey optic nerve. *Invest Ophthalmol Vis Sci.* 1986; **27**: 1342-50
164. Quigley HA, Addicks EM, Green R. Optic nerve damage in human glaucoma. III. Quantitative correlation of nerve fibre loss and visual field defect in glaucoma, ischaemic neuropathy, papilloedema and toxic neuropathy. *Arch. Ophthalmol.* 1982; **100**: 135-46



165. Martin PR, White AJR, Goodchild AK, Wilder HD, Sefton AE. Evidence that Blue-On cells are part of the third geniculocortical pathway in primates. *Eur J Neurosci.* 1997; **9**: 1536-41
166. White AJR, Wilder HD, Goodchild AK, Sefton J, Martin PR. Segregation of receptive field properties in the lateral geniculate nucleus of a new-world monkey, the marmoset *Callithrix jacchus*. *J Neurophysiol.* 1998; **80**: 2063-76
167. de Monasterio FM. Asymmetry of on- and off- pathways of blue-sensitive cones of the retina of macaques. *Brain Res.* 1979; **166**: 39-48
168. Teesalu P, Airaksinen PJ, Tuulonen A, Nieminen H, Alanko H. Fluorometry of the crystalline lens for correcting blue-on-yellow perimetry results. *Invest Ophthalmol Vis Sci.* 1997; **38**: 697-703
169. Sample PA, Martinez GA, Weinreb RN. Short-wavelength automated perimetry without lens density testing. *Am J Ophthalmol.* 1994; **118**: 632-41
170. De Jong LA Snepvangers CE, van den Berg TJ, Langerhorst CT. Blue-yellow perimetry in the detection of early glaucomatous damage. *Doc Ophthalmol.* 1990; **75**: 303-14
171. Hart WM Jr, Silverman SE, Trick GL, Nesher R, Gordon MO. Glaucomatous visual field damage. Luminance and color-contrast sensitivities. *Invest Ophthalmol Vis Sci.* 1990; **31**: 359-67
172. Sample PA, Bosworth CF, Blumenthal EZ, Gidein G, Weinreb RN. Visual Function-Specific Perimetry for Indirect Comparison of Different Ganglion Cell Populations in Glaucoma. *Invest Ophthalmol Vis Sci.* 2000; **41**: 1783-90
173. Johnson CA, Brandt JD, Khong AM, Adams AJ. Short-wavelength automated perimetry in low-, medium-, and high-risk ocular hypertensive eyes. Initial baseline results. *Arch Ophthalmol.* 1995; **113**: 70-6

174. Demirel S, Johnson C. Incidence and Prevalence of Short Wavelength Automated Perimetry Deficits in Ocular Hypertensive Patients. *Am J Ophthalmol.* 2001; **131**: 709-15
175. Johnson CA, Adams AJ, Casson EJ, Brandt JD. Blue-on-yellow perimetry can predict the development of glaucomatous visual field loss. *Arch Ophthalmol.* 1993; **111**: 645-50
176. Chaturvedi N, Hedley-Whyte ET, Dreyer EB. Lateral geniculate nucleus in glaucoma. *Am J Ophthalmol.* 1993; **116**: 182-8
177. Maddess T, Hemmi JM, James AC. Evidence for spatial aliasing effects in the Y-like cells of the magnocellular visual pathway. *Vision Res.* 1992; **38**: 1843-59
178. Kelly DH. Frequency doubling in visual responses. *J Opt Soc Am.* 1966; **56**: 1628-33
179. Kaplan E, Shapley RM. X and Y cells in the lateral geniculate nucleus of macaque monkeys. *J Physiol.* 1982; **330**: 125-43.
180. Maddess T, Henry GH. Performance of nonlinear visual units in ocular hypertension and glaucoma. *Clin Vis Sci.* 1992; **7**: 371-83
181. Quigley HA. Identification of glaucoma-related visual field abnormality with the screening protocol of frequency doubling technology. *Am J Ophthalmol.* 1998; **125**: 819-29
182. Johnson CA, Samuels SJ. Screening for glaucomatous visual field loss with frequency-doubling perimetry. *Invest Ophthalmol Vis Sci.* 1997; **38**: 413-25
183. Maddess T, Severt WL. Testing for glaucoma with frequency-doubling illusion in the whole, macular and eccentric visual fields. *Aust NZ J Ophthalmol.* 1999; **27**: 194-6
184. Victor JD, Shapley RM. The nonlinear pathway of Y ganglion cells in the cat retina. *J Gen Physiol.* 1979; **74**: 671-89

185. Shapley RM, Victor JD. The effect of contrast on the transfer properties of cat retinal ganglion cells. *J Physiol.* 1978; **285**: 275-98
186. Solomon SG, White AJR, Martin PR. Temporal contrast sensitivity in the lateral geniculate nucleus of a new world monkey, the marmoset *Callithrix jacchus*. *J Physiol.* 1999; **517**: 907-17
187. Johnson C, Wall M, Fingeret M *et al.* *A primer for frequency doubling technology*. Dublin, CA, USA: Humphrey Systems Welch-Allyn, Inc. 1998
188. Lachenmayr BJ, Gleissner M. Flicker perimetry resists retinal image degradation. *Invest Ophthalmol Vis Sci.* 1992; **33**: 3539-42
189. Anderson AJ, Johnson CA. Frequency-Doubling Technology Perimetry and Optical Defocus. *Invest Ophthalmol Vis Sci.* 2003; **44**: 4147-52
190. Artes PH, Nicolela MT, McCormick TA, LeBlanc RP, Chauhan BC. Effects of Blur and Repeated Testing on Sensitivity Estimates with Frequency Doubling Perimetry. *Invest Ophthalmol Vis Sci.* 2003; **44**: 646-52
191. Ito A, Kawabata H, Fujimoto N, Adachi-Usami E. Effect of myopia on frequency-doubling perimetry. *Invest Ophthalmol Vis Sci.* 2001; **42**: 1107-10
192. Heeg GP, Ponsioen TL, Jansonius NM. Learning Effect, Normal Range, and Test-Retest Variability of Frequency Doubling Perimetry as a Function of Age, Perimetry Experience, and the Presence or Absence of Glaucoma. *Ophthalm Physiol Opt.* 2003; **23**: 535-40
193. Matsuo H, Tomita G, Suzuki Y, Araie M. Learning Effect and Measurement Variability in Frequency-Doubling Technology Perimetry in Chronic Open-Angle Glaucoma. *J Glaucoma.* 2002; **11**: 467-73
194. Brusini P, Busatto P. Frequency doubling perimetry in glaucoma early diagnosis. *Acta Ophthalmol Scand.* 1998; **227**: 23-4

195. Chauhan BC, Johnson CA. Test-retest Variability Characteristics of Frequency Doubling Perimetry and Conventional Perimetry in Glaucoma Patients and Normal Controls. *Invest Ophthalmol Vis Sci.* 1999; **40**: 648-56
196. Sponsel WE, Argango S, Trigo Y, Cot Mensah J. Clinical classification of glaucomatous visual field loss by frequency doubling perimetry. *Am J Ophthalmol.* 1998; **125**: 830-6
197. Cello KE, Nelson-Quigg JM, Johnson CA. Frequency Doubling Technology Perimetry For Detection of Glaucomatous Visual Field Loss. *Am J Ophthalmol.* 2000; **129**: 314-22
198. Burnstein Y, Elish N, Magbalov M *et al.* Comparison of frequency doubling perimetry with Humphrey visual field analysis in a glaucoma practice. *Am J Ophthalmol* 2000; **129**: 328-33
199. Tribble JR, Schultz RO, Robinson JC, Rothe TL. Accuracy of glaucoma detection with frequency-doubling perimetry. *Am J Ophthalmol.* 2000; **129**: 740-5
200. Casson EJ, Johnson CA, Shapiro LR. Longitudinal comparison of temporal-modulation perimetry with white-on-white and blue-on-yellow perimetry in ocular hypertension and early glaucoma. *J. Opt. Soc. Am.* 1993; **10**: 1792-806
201. Landers J, Goldberg I, Graham S. A comparison of short wavelength automated perimetry with frequency doubling perimetry for the early detection of visual field loss in ocular hypertension. *Clin Experiment Ophthalmol.* 2000; **28**: 248-52
202. Bayer AU, Erb C. Short Wavelength Automated Perimetry, Frequency Doubling Technology Perimetry, and Pattern Electroretinography for Prediction of Progressive Glaucomatous Standard Visual Field Defects. *Ophthalmology.* 2002; **109**: 1009-17
203. Rota-Bartelink A, Pitt A, Story I, Rait J. Automated flicker perimetry in early primary open-angle glaucoma. *Aust NZ J Ophthalmol.* 1996; **24**[Suppl]: 25-7

204. Soliman MAE, de Jong LA, Ismaeil AA, van den Berg TJ, de Smet MD. Standard Achromatic Perimetry, Short Wavelength Automated Perimetry, and Frequency Doubling Technology for Detection of Glaucoma Damage. *Ophthalmology*. 2002; **109**: 444-54
205. Kondo Y, Yamamoto T, Sato Y, Matsubara M, Kitazawa Y. A frequency-doubling perimetric study in normal-tension glaucoma with hemifield defect. *J Glaucoma*. 1998; **7**: 261-5
206. Wu LL, Suzuki Y, Kunimatsu S, Araie M, Iwase A, Tomita G. Frequency doubling technology and confocal scanning ophthalmoscopic optic disc analysis in open-angle glaucoma with hemifield defects. *J Glaucoma*. 2001; **10**: 256-60
207. Austin MW, O'Brien CJ, Wishart PK. Flicker perimetry using a luminance threshold strategy at frequencies from 5-25 Hz in glaucoma, ocular hypertension and normal controls. *Curr Eye Res*. 1994; **13**: 717-23
208. Horn FK, Wakili N, Junemann AM, Korth M. Testing for glaucoma with frequency-doubling perimetry in normals, ocular hypertensives, and glaucoma patients. *Graefes Arch Clin Exp Ophthalmol*. 2002; **240**: 658-65
209. Medeiros FA, Sample PA, Weinreb RN. Corneal thickness measurements and frequency doubling technology perimetry abnormalities in ocular hypertensive eyes. *Ophthalmology*. 2003; **110**: 1903-8
210. Kalaboukhova L, Lindblom B. Frequency doubling technology and high-pass resolution perimetry in glaucoma and ocular hypertension. *Acta Ophthalmol (Scand)*. 2003; **81**: 247-52
211. Drance SM. The Evolution of Perimetry. In: Whalan WR, Spaeth G (eds) *Computerized Visual Fields: What They Are and How We Use Them*. Thorofare NJ: SLACK Inc., 1985

212. Johnson CA, Keltner JL, Balestrery FG. Suprathreshold static perimetry in glaucoma and other optic nerve disease. *Ophthalmology* 1979; **86**: 1278-86
213. Demirel S, Johnson CA. Short wavelength automated perimetry (SWAP) in ophthalmic practice. *J Am Opt Assoc.* 1996; **67**: 451-6
214. Caprioli J. Automated perimetry in glaucoma. *Am J Ophthalmol.* 1991; **111**: 235-9
215. Perez JS, Bosworth CF, Weinreb RN. Frequency doubling threshold perimetry (FDP) in glaucoma and glaucoma suspect eyes. ARVO. Abstracts. *Invest Ophthalmol Vis Sci.* 1998; **109**: S26
216. Sample PA, Johnson CA, Haegerstrom-Portnoy G, Adams AJ. Optimum parameters for short-wavelength automated perimetry. *J. Glaucoma* 1996; **5**: 375-83
217. Kaplan E, Shapley RM. The primate retina contains two types of ganglion cells, with high and low contrast sensitivity. *Proc Natl Acad Sci USA.* 1986; **83**: 2755-7
218. Bedford S, Maddess T, Rose KA, James AC. Correlations between observability of the spatial frequency doubling illusion and a multi-region pattern electroretinogram. *Aust NZ J Ophthalmol.* 1997; **25**: 591-3
219. Maddess T, Goldberg I, Dobinson J, Wine S, Welsh AH, James AC. Testing for glaucoma with the spatial frequency doubling illusion. *Vision Res.* 1999; **39**: 4358-73
220. Walker WM. Ocular hypertension. Follow-up of 109 cases from 1963 to 1974. *Trans Ophthalmol Soc.* 1974; **94**: 525-34
221. Kitazawa Y, Horie T, Aoki S, Suzuki M, Nishioka K. Untreated ocular hypertension. A long-term prospective study. *Arch Ophthalmol.* 1977; **95**: 1180-4

222. Sommer A, Pollack I, Maumenee AE. Optic disc parameters and onset of glaucomatous field loss. Methods and progressive changes in disc morphology. *Arch Ophthalmol.* 1979; **97**: 1444-8
223. Von Graefe A. Vorläufige notiz über das wesen des glaucoms. *Arch Ophthalmol.* 1854; **1**: 371-4
224. Radius R. Anatomy of the optic nerve head and glaucomatous optic neuropathy. *Surv Ophthalmol.* 1987; **32**: 35-44
225. Quigley HA, Addicks EM, Green R, Maumenee AE. Optic nerve damage in human glaucoma. II. The site of injury and susceptibility to damage. *Arch Ophthalmol.* 1981; **99**: 635-47
226. Motolko M, Drance SM. Features of the optic disc in preglaucomatous eyes. *Arch Ophthalmol.* 1981; **99**: 1992-4
227. Garway-Heath DF, Ruben ST, Viswanathan A, Hitchings RA. Vertical cup/disc ratio in relation to optic disc size: its value in the assessment of the glaucoma suspect. *Br J Ophthalmol.* 1998; **82**: 1118-24
228. Odberg T, Riise D. Early diagnosis of glaucoma. The value of successive stereophotography of the optic disc. *Acta Ophthalmol.* 1985; **63**: 257-63
229. Miglor S, Brigatti L, Lonati C, Rossetti L, Pierrottet C, Orzalesi N. Correlation between the progression of optic disc and visual field changes in glaucoma. *Curr Eye Res.* 1996; **15**: 145-50
230. Damms T, Dannhein F. Sensitivity and specificity of optic disc parameters in chronic glaucoma. *Invest Ophthalmol Vis Sci.* 1993; **34**: 2246-50
231. Gloster J. Quantitative relationship between cupping of the optic disc and visual field loss in chronic simple glaucoma. *Br J Ophthalmol.* 1978; **62**: 665-9

232. Jonas JB, Bergua A, Schmitz-Valckenberg P, Papastathopoulos KI, Budde WM. Ranking of optic disc variables for detection of glaucomatous optic nerve damage. *Invest Ophthalmol Vis Sci.* 2000; **41**: 1764-73
233. Kerrigan-Baumrind LA, Quigley HA, Pease ME, Kerrigan DF, Mitchell RS. Number of ganglion cells in glaucoma eyes compared with threshold visual field tests in some persons. *Invest Ophthalmol Vis Sci.* 2000; **41**: 741-8
234. Polo V, Larrosa JM, Pablo LE, Piaila I, Honrubia F. Correlation of functional and structural measurements in eyes suspected of having glaucoma. *J Glaucoma.* 1999; **8**: 172-6
235. Polo V, Abecia E, Pablo LE, Pinilla I, Larrosa JM, Honrubia FM. Short wavelength automated perimetry and retinal nerve fibre layer evaluation in suspected case of glaucoma. *Arch Ophthalmol.* 1998; **116**: 1295-8
236. Tsai CS, Zangwill L, Sample PA, Gordon V, Bartsch D-U, Weinreb RN. Correlation of peripapillary retinal height and visual field in glaucoma and normal subjects. *J Glaucoma.* 1995; **4**: 110-16
237. Kass MA, Gordon MO, Hoff MR *et al.* Topical timolol administration reduces the incidence of glaucomatous damage in ocular hypertensive individuals. *Arch Ophthalmol.* 1989; **107**: 1590-98
238. Epstein DL, Krug JH, Hertzmark E, Remis LL, Edelstein DJ. A long-term clinical trial of timolol therapy versus no treatment in the management of glaucoma suspects. *Ophthalmology.* 1989; **96**: 1460-7
239. Collaborative Normal-Tension Glaucoma Study Group. Comparison of glaucomatous progression between untreated patients with normal-tension glaucoma and patients with therapeutically reduced intraocular pressures. *Am J Ophthalmol.* 1998; **126**: 487-97



240. O'Connor P, Zeyen T, Caprioli J. Comparisons of methods to detect glaucomatous optic nerve damage. *Ophthalmology*. 1993; **100**: 1498-503
241. Wild JM, Cubbidge RP, Pacey IE, Robinson R. Statistical aspects of the normal visual field in short-wavelength automated perimetry. *Invest Ophthalmol Vis Sci*. 1998; **39**: 54-63
242. Johnson CA, Cioffi GA, Van Buskirk EM. Frequency doubling technology perimetry using a 24-2 stimulus presentation pattern. *Optom Vis Sci*. 1999; **76**: 571-81
243. Vingrys AJ, Helfrich KA. The Opticom M600: a new LED automated perimeter. *Clin Exp Opt*. 1990; **73**: 3-17
244. Pye D, Herse P, Nguyen H, et al. Conversion factor for comparison of data from Humphrey and Medmont automated perimeters. *Clin Exp Opt*. 1999; **82**: 11-13
245. McKendrick AM, Vingrys AJ, Badcock DR, et al. Visual field losses in subjects with migraine headaches. *Invest Ophthalmol Vis Sci*. 2000; **41**: 1239-47
246. Graham SL, Drance SM, Chauhan BC, et al. Comparison of psychophysical and electrophysiological testing in early glaucoma. *Invest Ophthalmol Vis Sci*. 1996; **37**: 2651-62
247. Johnson CA. Selective Versus Nonselective Losses in Glaucoma. *J Glaucoma*. 1994; **3 [Suppl 1]**: S32-S44
248. Yucel YH, Zhang Q, Gupta N, Kaufman PL, Weinreb RN. Loss of Neurons in Magnocellular and Parvocellular Layers of the Lateral Geniculate Nucleus in Glaucoma. *Arch Ophthalmol*. 2000; **118**: 378-84
249. Iester M, Altieri M, Vittone P, Calabria G, Zingirian M, Traverso CE. Detection of Glaucomatous Visual Field Defect by Nonconventional Perimetry. *Am J Ophthalmol*. 2003; **135**: 35-9

250. Martin L, Wauger P, Vancea L, Göthlin B. Concordance of High-Pass Resolution Perimetry and Frequency Doubling Technology Perimetry Results in Glaucoma: No Support for Selective Ganglion Cell Damage. *J Glaucoma*. 2003; **12**: 40-44
251. White AJ, Sun H, Swanson WH, Lee BB. An Examination of Physiological Mechanisms Underlying the Frequency-Doubling Illusion. *Invest Ophthalmol Vis Sci*. 2002; **43**: 3590-9
252. Anderson AJ, Johnson CA. Mechanisms Isolated by Frequency-Doubling Technology Perimetry. *Invest Ophthalmol Vis Sci*. 2002; **43**: 398-401
253. Iester M, Mermoud A, Schnyder C. Frequency Doubling Technique in Patients with Ocular Hypertension and Glaucoma. *Ophthalmology*. 2000; **107**: 288-94
254. Dacey DM, Lee BB. The "Blue-On" Opponent Pathway in Primate Retina Originates from a Distinct Bistratified Ganglion Cell Type. *Nature*. 1994; **367**: 731-5
255. Harbin TS Jr, Podos SM, Koller AE, Becker B. Visual Field Progression in Open-Angle Glaucoma Patients Presenting with Monocular Field Loss. *Trans Am Acad Ophthalmol Otolaryngol*. 1976; **81**: 253-7
256. Fontana L, Armas R, Garway-Heath DF, Bunce CV, Poinoosawmy D, Hitchings RA. Clinical Factors Influencing the Visual Prognosis of the Fellow Eyes of Normal Tension Glaucoma Patients with Unilateral Field Loss. *Br J Ophthalmol*. 1999; **83**: 1002-5
257. Shapley R, Enroth-Cugell C. Visual adaptation and retinal gain controls. In, Osborne NN, Chader GJ, eds. *Prog Ret Res*. Oxford: Pergamon Press 1982; **3**: 263-343
258. Aulhorn E. Über die Beziehung Zwischen Lichtsinn und Sehschärfe. *Albrecht Von Graefes Arch Ophthalmol*. 1964; **167**: 4-74

259. Johnson CA, Kelter JL, Balestrery F. Effects of target size and eccentricity on visual detection and resolution. *Vis Res.* 1978; **18**: 1217-22
260. Wassle H, Grunert U, Rohrenbeck J *et al.* Retinal ganglion cell density and cortical magnification factor in the primate. *Vis Res.* 1990; **30**: 1897-911
261. Anderson DR. *Perimetry With and Without Automation. 2nd ed.* St Louis: CV Mosby, 1987
262. Merigan WH, Katz LM, Maunsell JHR. The effects of parvocellular lateral geniculate lesions on the acuity and contrast sensitivity of macaque monkeys. *J Neuroscience* 1991; **11**: 944-1001
263. Sample PA, Irak I, Martinez GA *et al.* Asymmetries in the normal short-wavelength visual field: implications for short-wavelength automated perimetry. *Am J Ophthalmol* 1997; **124**: 46-52
264. Johnson CA, Adams AJ, Twelker JD *et al.* Age-related changes in the central visual field for short-wavelength-sensitive pathways. *J Opt Soc Am.* 1988; **5**: 2131-9
265. Livingstone MS, Hubel DH. Do the relative mapping densities of the magno-and parvocellular systems vary with eccentricity? *J Neuroscience.* 1988; **8**: 4334-9
266. Jacobs NA, Patterson IH. Variability of the hill of vision and its significance in automated perimetry. *Brit J Ophthalmol.* 1985; **69**: 824-6
267. Heijl A, Lindgren G, Olsson J. Normal variability of static perimetric threshold values across the central visual field. *Arch Ophthalmol.* 1987; **105**: 1544-9
268. Parrish RK, Schiffman J, Anderson DA. Static and kinetic visual field testing. reproducibility in normal volunteers. *Arch Ophthalmol.* 1984; **102**: 1497-1502
269. Foster PJ, Buhrmann R, Quigley HA *et al.* The definition and classification of glaucoma in prevalence surveys. *Br J Ophthalmol.* 2002; **86**: 238-42

270. House P, Schulzer M, Drance S *et al.* Characteristics of the normal central visual field measured with resolution perimetry. *Graefes Arch Clin Exp Ophthalmol.* 1991; **229**: 8-12
271. Wall M, Chauhan B, Frisén L *et al.* Visual field of high-pass resolution perimetry in normal subjects. *J Glaucoma.* 2004; **13**: 15-21
272. Wojciechowski R, Trick GL, Steinman SB. Topography of the age-related decline in motion sensitivity. *Opt Vis Sci.* 1995; **72**: 67-74
273. Connolly M, Van Essen D. The representation of the visual field in parvocellular and magnocellular layers in the lateral geniculate nucleus in the macaque monkey. *J Comp Neurol.* 1984; **226**: 544-64
274. Adams CW, Bullimore MA, Wall M *et al.* Normal aging effects for frequency doubling technology perimetry. *Opt Vis Sci.* 1999; **76**: 582-7
275. Landers J, Goldberg I, Graham S. Detection of Early Visual Field Loss in Glaucoma Using Frequency Doubling Perimetry and Short Wavelength Automated Perimetry. *Arch Ophthalmol.* 2003; **121**: 1705-10
276. Iwasaki A, Sugita M. Performance of glaucoma mass screening with only a visual field test using frequency-doubling technology perimetry. *Am J Ophthalmol.* 2002; **134**: 529-37
277. Khong JJ, Dimitrov PN, Rait J, McCarty CA. Can the specificity of the FDT for glaucoma be improved by confirming abnormal results? *J Glaucoma.* 2001; **10**: 199-202
278. Casson R, James B, Rubinstein A, Ali H. Clinical comparison of frequency doubling technology perimetry and Humphrey perimetry. *Brit J Ophthalmol.* 2001; **85**: 360-2

279. Cioffi GA, Mansberger S, Spry P, Johnson C, Van Buskirk EM. Frequency doubling perimetry and the detection of eye disease in the community. *Trans Am Ophthalmol Soc.* 2000; **98**: 195-9
280. Patel SC, Friedman DS, Varadkar P, Robin AL. Algorithm for interpreting the results of frequency doubling perimetry. *Am J Ophthalmol.* 2000; **129**: 323-7
281. Muskens RP, Heeg GP, Jansonius NM. An evaluation of algorithms designed to classify the results from frequency doubling perimetry. *Ophthal Physiol Opt.* 2004; **24**: 498-503
282. Bowd C, Zangwill LM, Berry CC, Blumenthal EZ, Vasile C *et al.* Detecting Early Glaucoma by Assessment of Retinal Nerve Fiber Layer Thickness and Visual Function. *Invest Ophthalmol Vis Sci.* 2001; **42**: 1993-2003
283. Thomas R, Bhat S, Muliyl JP, Parikh R, George R. Frequency Doubling Perimetry in Glaucoma. *J Glaucoma.* 2002; **11**: 46-50
284. Yamada N, Chen PP, Mills RP, Leen MM, Lieberman MF *et al.* Screening for Glaucoma with Frequency-Doubling Technology and Damato Campimetry. *Arch Ophthalmol.* 1999; **117**: 1479-84
285. Katz J, Tielsch JM, Quigley HA, Sommer A. Automated perimetry detects visual field loss before manual Goldmann perimetry. *Ophthalmology.* 1995; **102**: 21-6
286. Moss ID, Wild JM, Whitaker DJ. The influence of age-related cataract on blue-on-yellow perimetry. *Invest Ophthalmol Vis Sci.* 1995; **36**: 764-73
287. Artes PH, Chauhan BC. Longitudinal changes in the visual field and optic disc in glaucoma. *Prog Ret Eye Res.* 2005; **24**: 333-54
288. Morgan JE, Uchida H, Caprioli J. Retinal ganglion cell death in experimental glaucoma. *Br J Ophthalmol.* 2000; **84**: 303-10
289. Weber AJ, Kaufman P, Hubbard WC. Morphology of single ganglion cells in the glaucomatous primate retina. *Invest Ophthalmol Vis Sci.* 1998; **39**: 2304-20

290. Ansari EA, Morgan JE, Snowden RJ. Psychophysical characterisation of early functional loss in glaucoma and ocular hypertension. *Br J Ophthalmol*. 2002; **86**: 1131-5
291. Garway-Heath DF, Caprioli J, Fitzke FW, Hitchings RA. Scaling the Hill of Vision: The Physiological Relationship between Light Sensitivity and Ganglion Cell Numbers. *Invest Ophthalmol Vis Sci*. 2000; **41**: 1774-1782
292. Garway-Heath DF, Holder GE, Fitzke FW, Hitchings RA. Relationship between Electrophysiological, Psychophysical, and Anatomical Measurements in Glaucoma. *Invest Ophthalmol Vis Sci*. 2002; **43**: 2213-2220
293. Tyler CW, Hardage L, Stamper RL. The temporal visuogram in ocular hypertension and its progression to glaucoma. *J Glaucoma*. 1994; **3**[Suppl]: S65-S72
294. Tyler CW. Specific deficits of flicker sensitivity on glaucoma and ocular hypertension. *Invest Ophthalmol Vis Sci*. 1981; **20**: 204-12
295. Yoshiyama KK, Johnson CA. Which method of flicker perimetry is most effective for detection of glaucomatous visual field loss? *Invest Ophthalmol Vis Sci*. 1997; **38**: 2270-2277
296. Kiryu J, Asrani S, Shahidi M, Mori M, Zeimer R. Local response of the primate retinal microcirculation to increased metabolic demand induced by flicker. *Invest Ophthalmol Vis Sci*. 1995; **36**: 1240-6
297. Riva CE, Falsini B, Logean E. Flicker-evoked responses of human optic nerve head blood flow: luminance versus chromatic modulation. *Invest Ophthalmol Vis Sci*. 2001; **42**: 756-62
298. Chauhan BC, Drance SM, Douglas GR. The use of visual field indices in detecting changes in the visual field in glaucoma. *Invest Ophthalmol Vis Sci*. 1990; **31**: 512-20

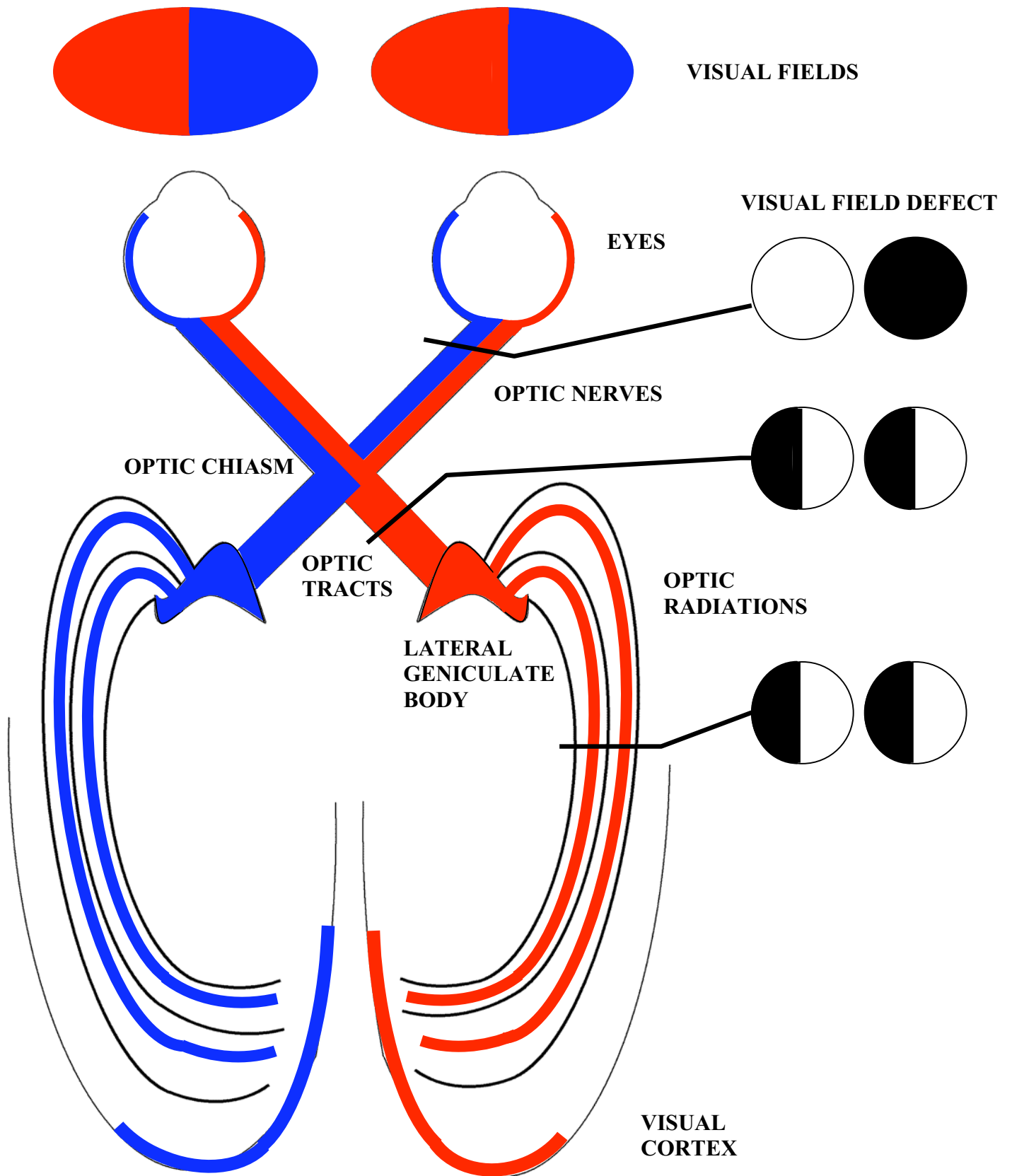


Figure 1. Visual pathways and visual field defects resulting from injury to the pathways

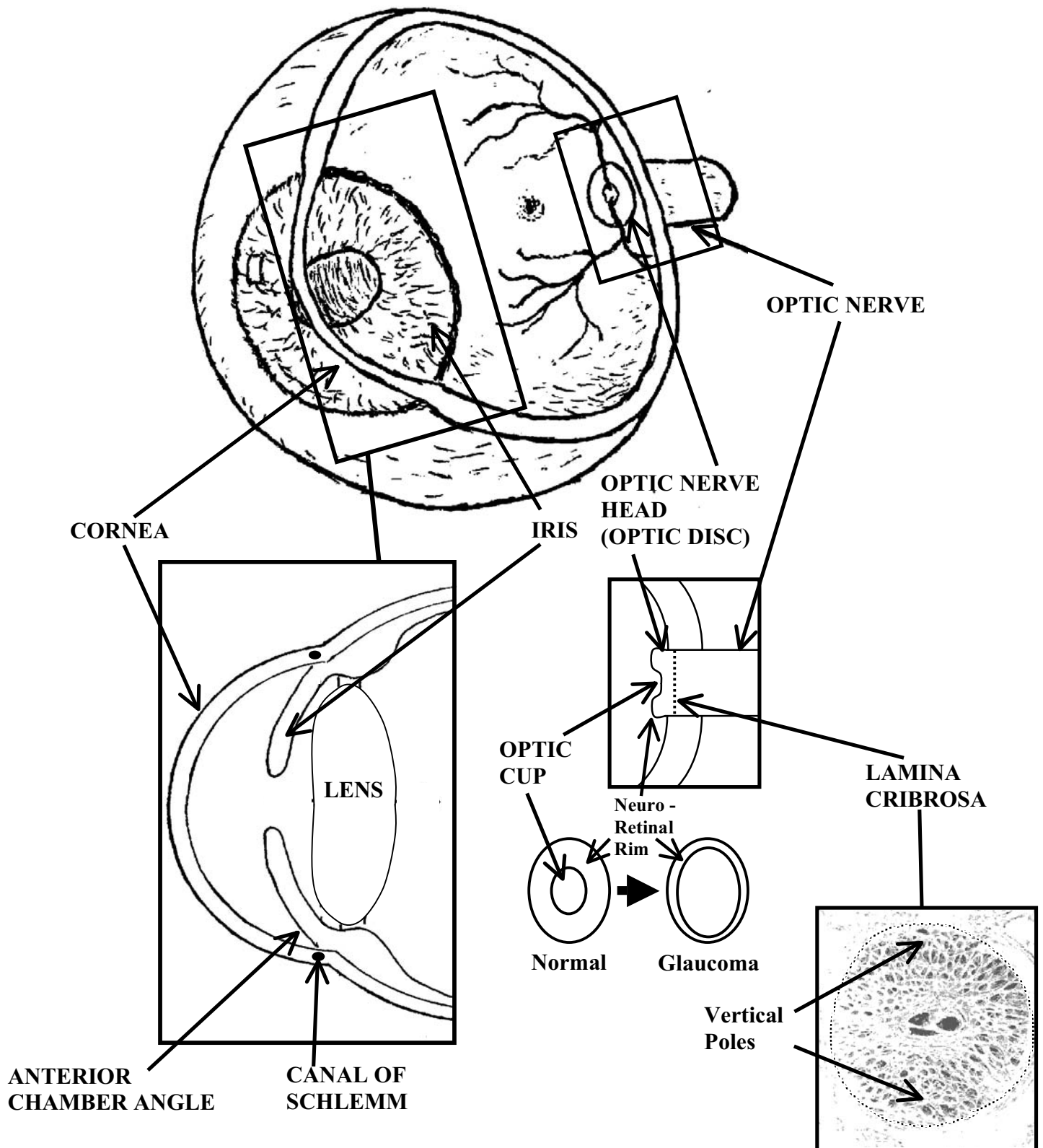


Figure 2. Schematic representation of the anatomy of the eye



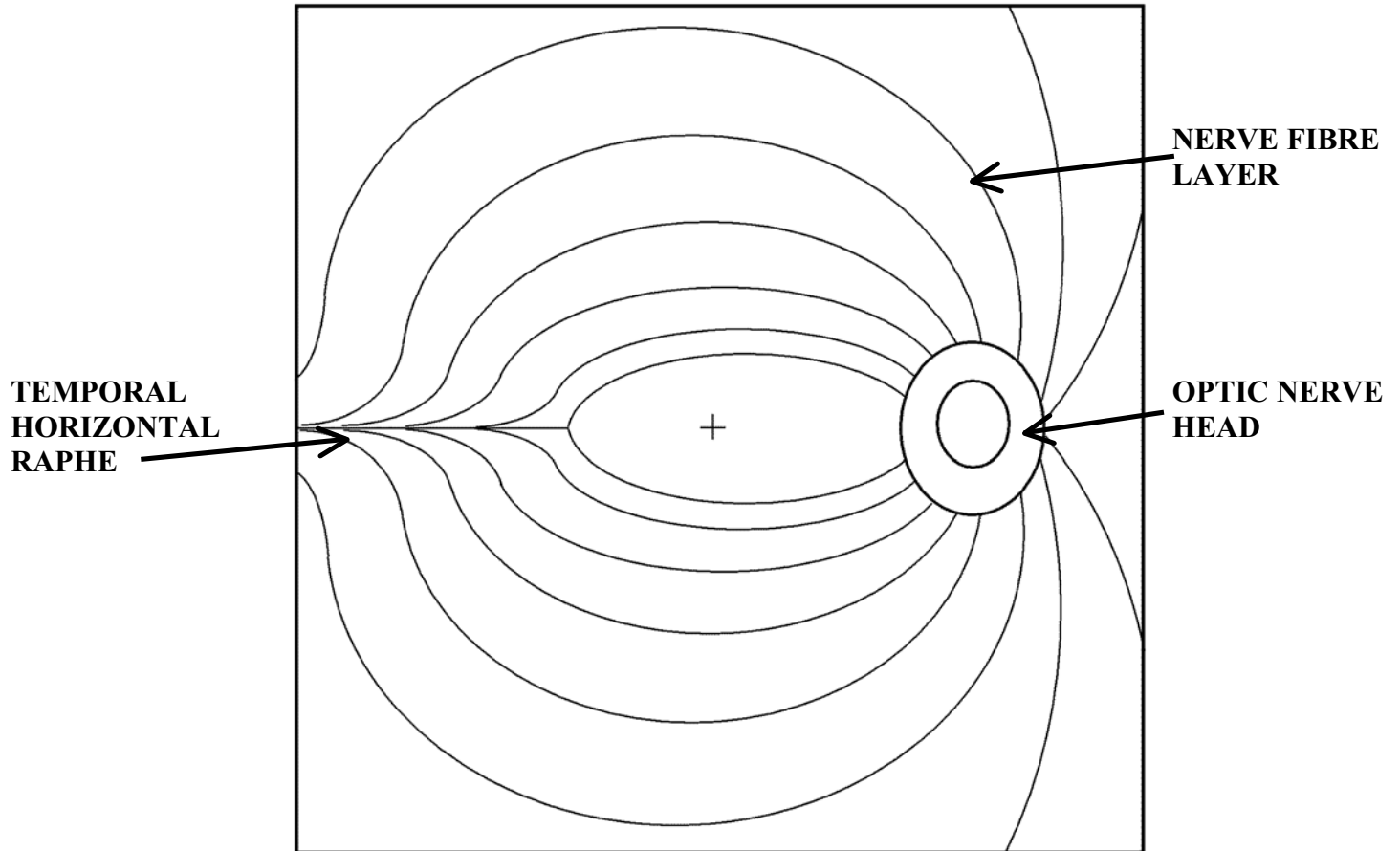


Figure 3. Schematic representation of the nerve fibre layer

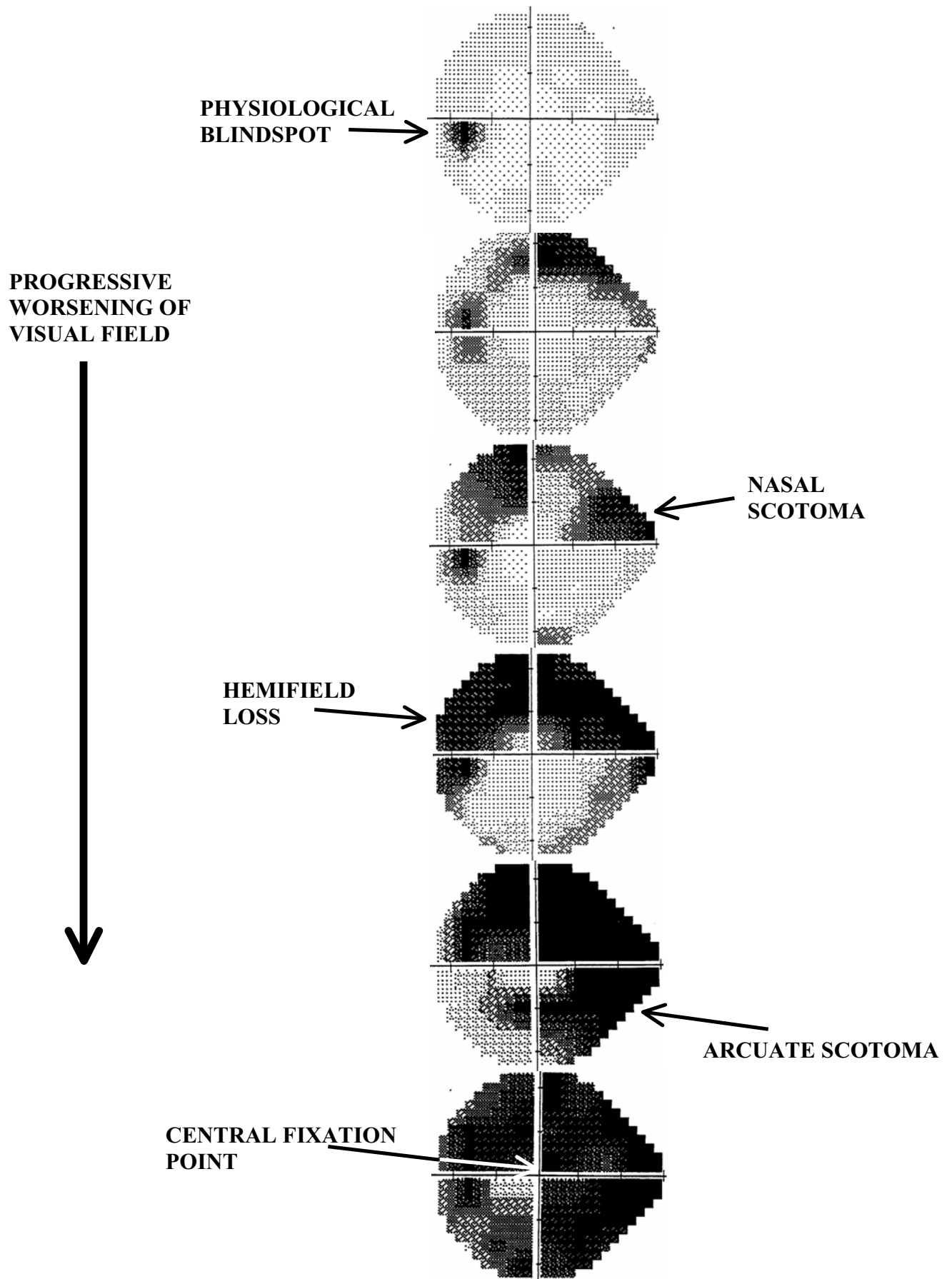


Figure 4. Grey-scale of the left visual field showing progressive loss from glaucoma

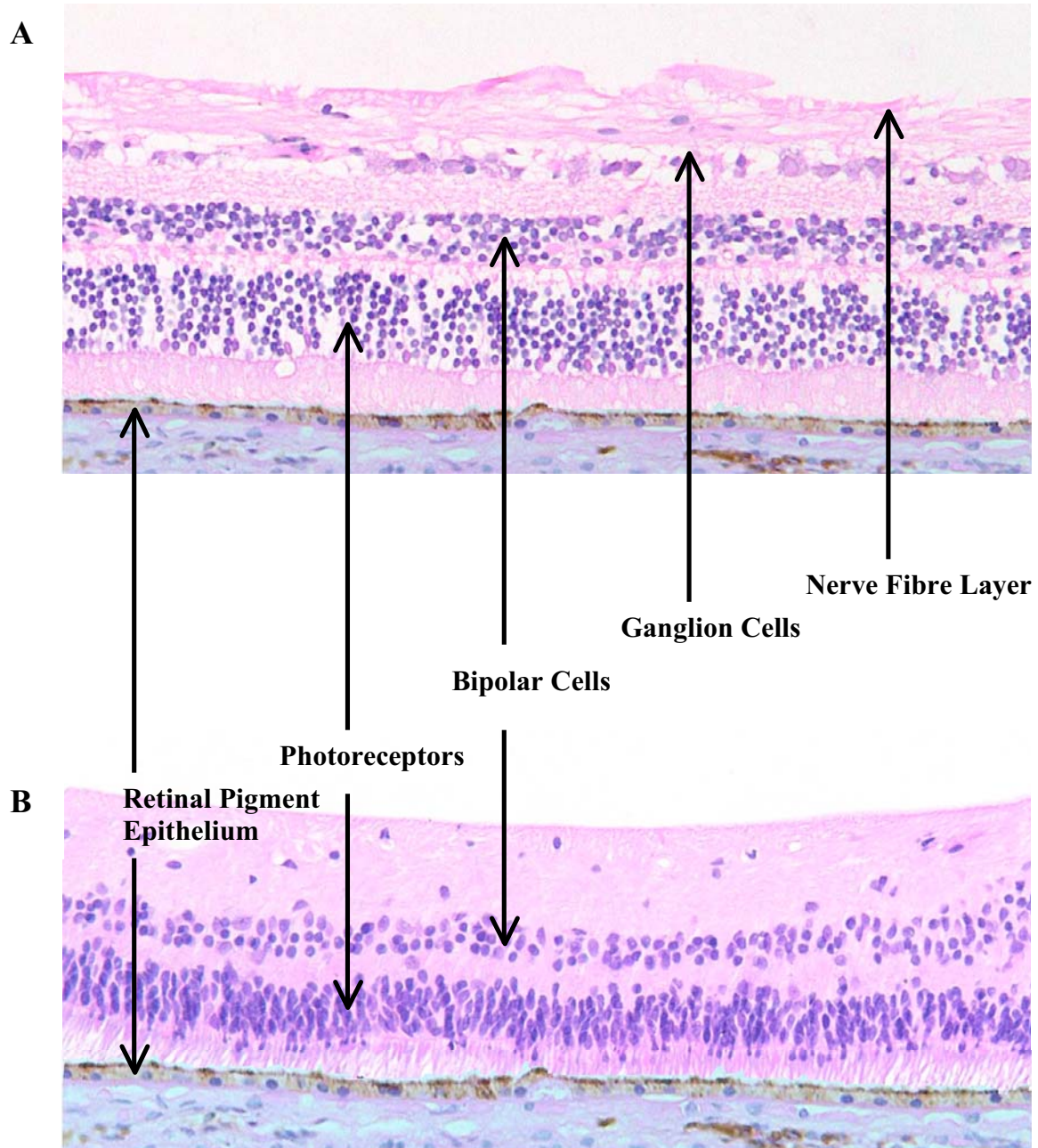


Figure 5. Micrograph of retina in (A) Healthy patient and (B) Glaucoma patient

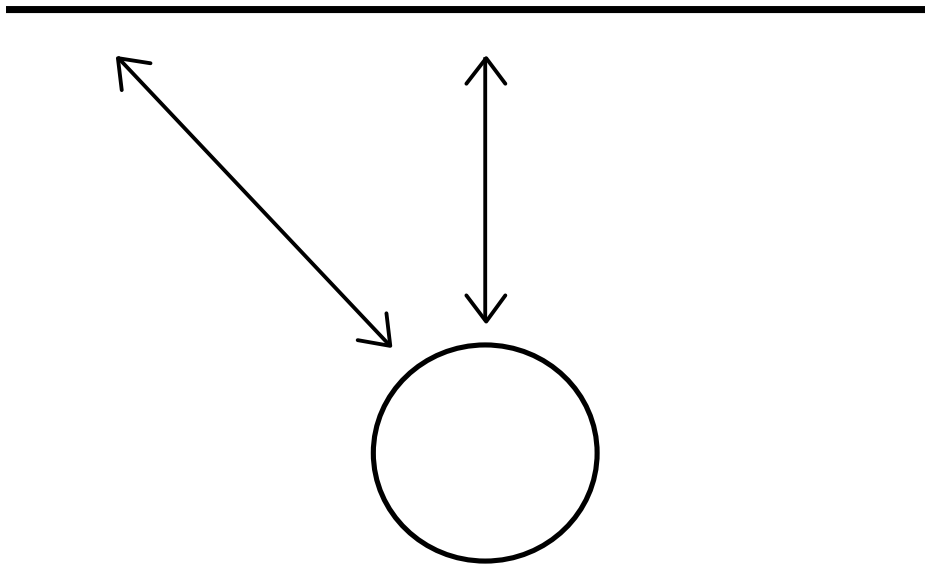


Figure 6. Schematic representation of visual field testing with a flat screen (campimetry)

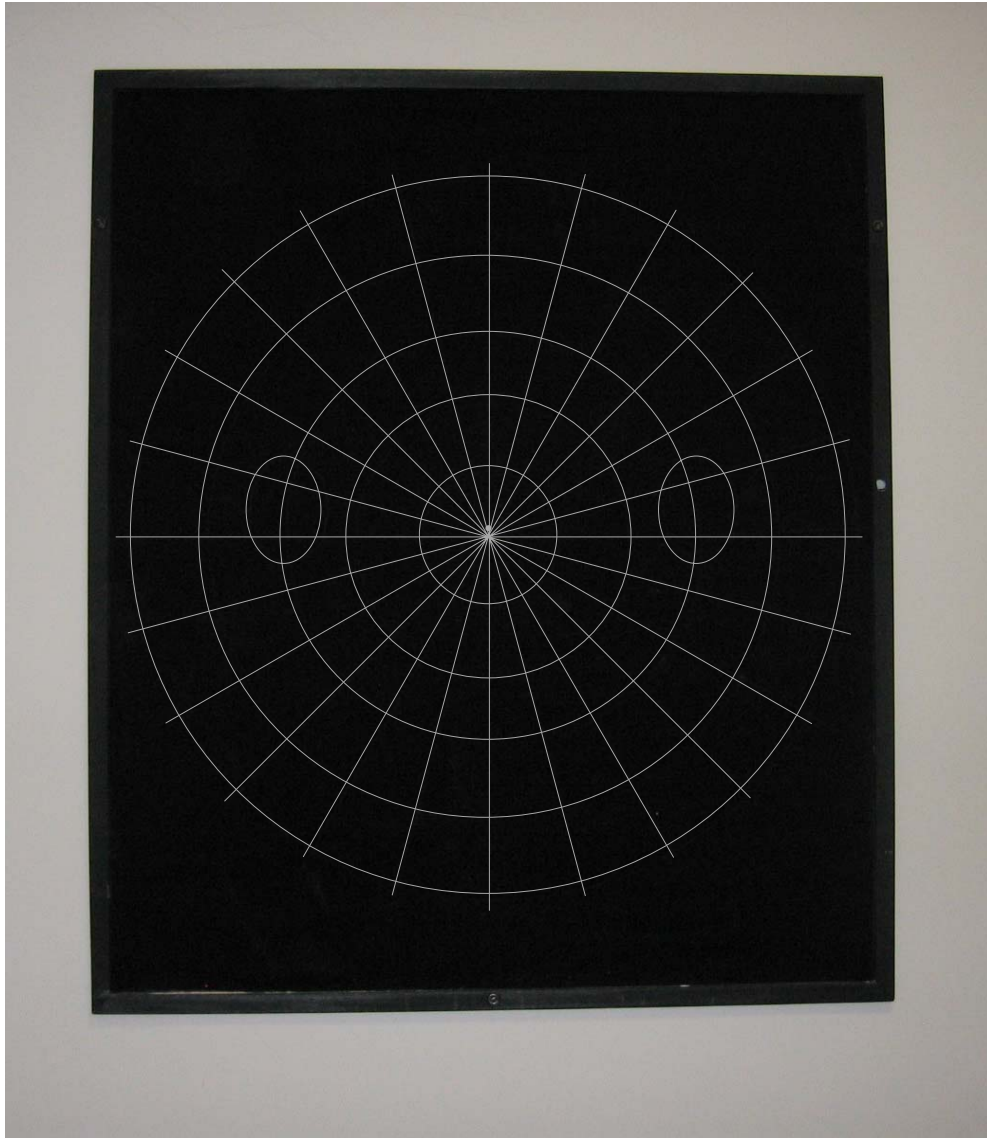


Figure 7. Bjerrum screen

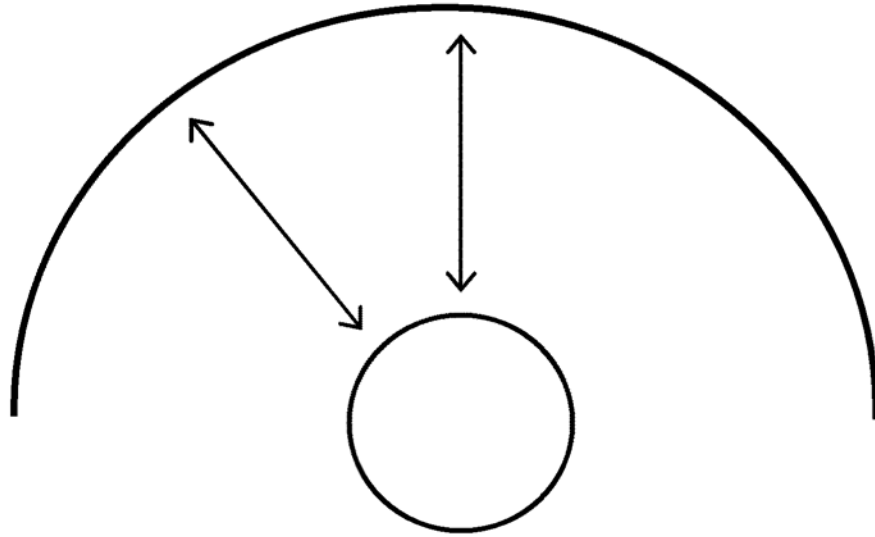


Figure 8. . Schematic representation of visual field testing with a curved screen (perimetry)

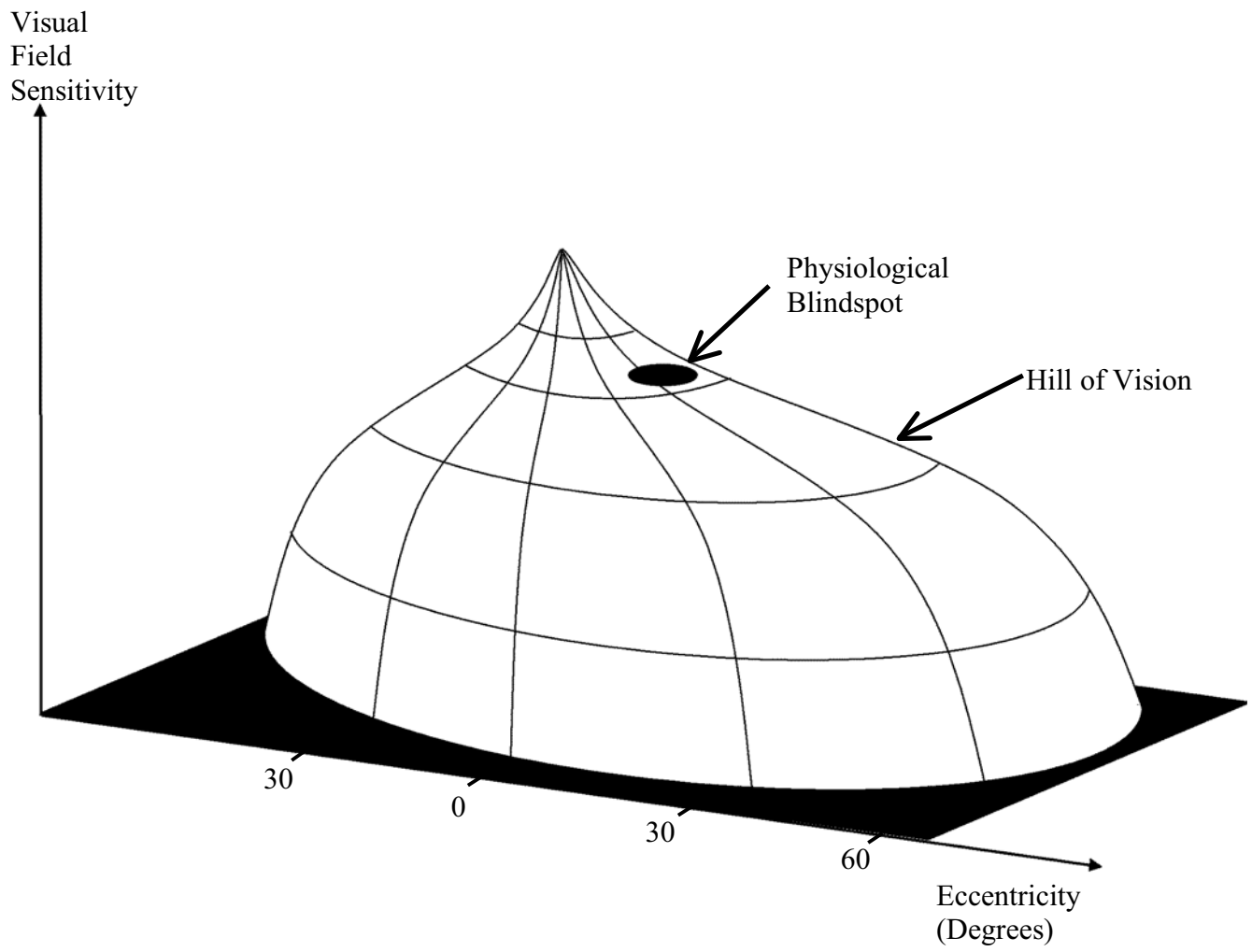


Figure 9. The 'Island of Traquair'



Figure 10 The Goldman Perimeter



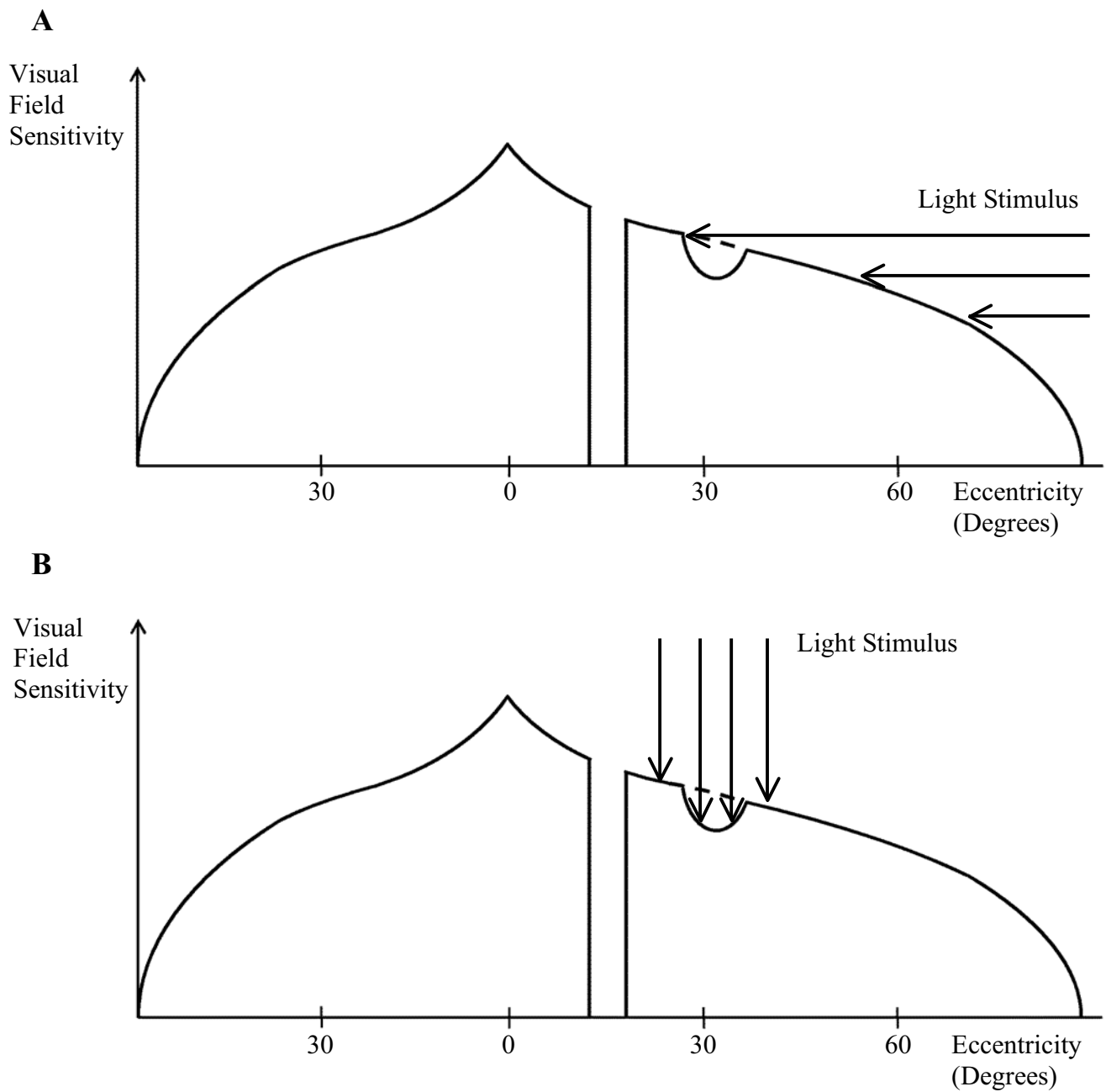


Figure 11 Mapping a small visual field scotoma using (A) kinetic and (B) static perimetry

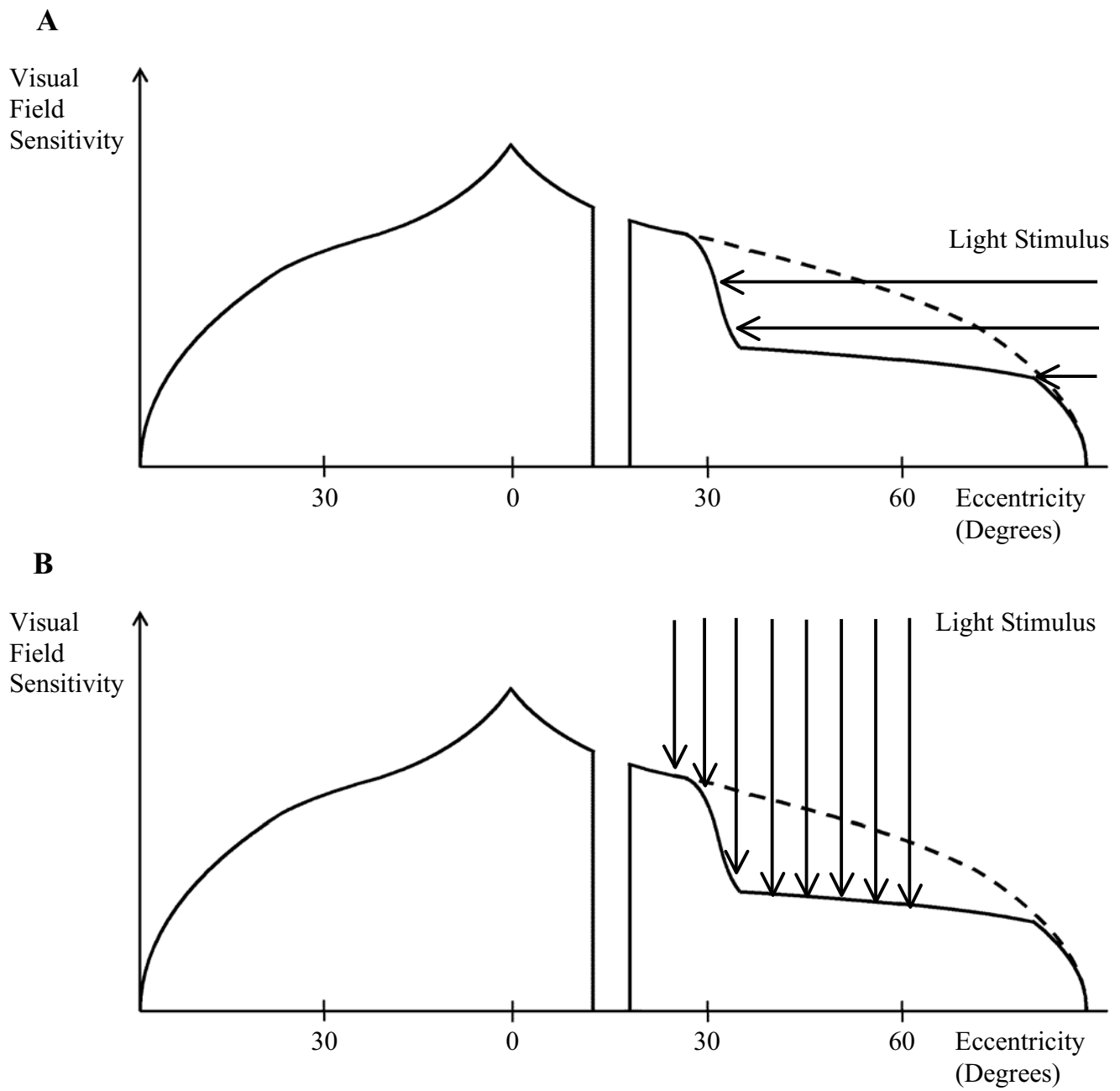


Figure 12 Mapping a steep scotoma using (A) kinetic and (B) static perimetry



Figure 13. The Humphrey Field Analyzer



Figure 14. The Medmont perimeter

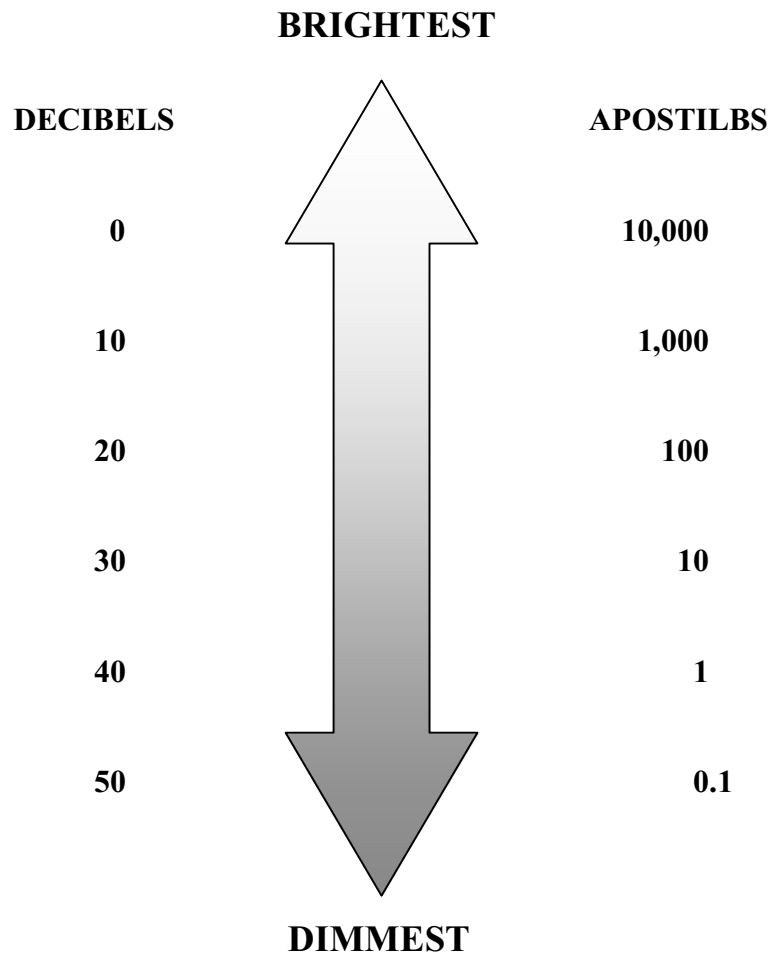


Figure 15. The relationship between stimulus brightness (Apostilbs) and visual field sensitivity (Decibels)

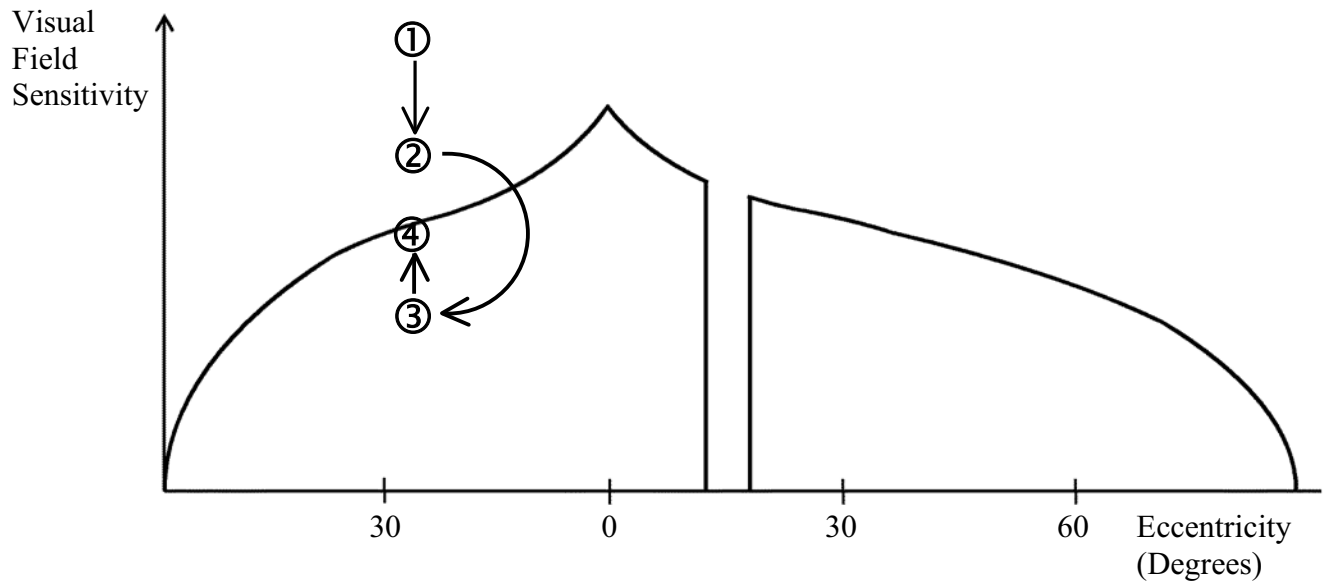


Figure 16. Schematic representation of the 'Stair-case' method used in static automated perimetry

Single Field Analysis

Eye: Right

Name: 064 ID: DOB: 25-04-1944

Central 24-2 Threshold Test

Fixation Monitor: Blindspot  
 Fixation Target: Central  
 Fixation Losses: 0/18  
 False POS Errors: 0/11  
 False NEG Errors: 0/9  
 Test Duration: 09:04

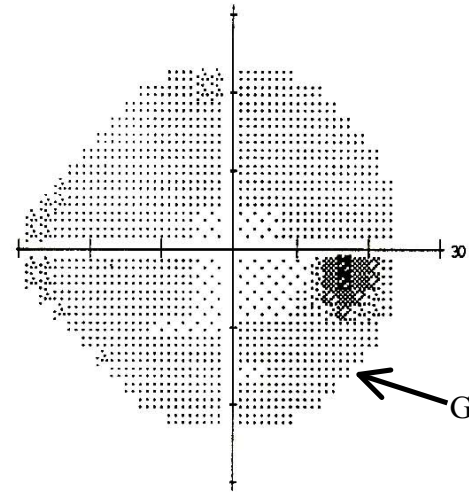
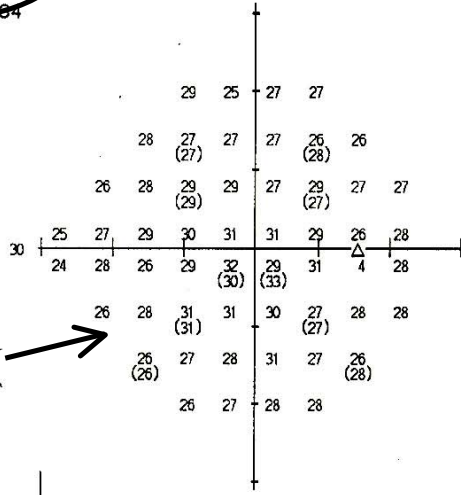
Stimulus: III, White  
 Background: 31.5 ASB  
 Strategy: Full Threshold

Pupil Diameter: 5.8 mm  
 Visual Acuity: 6/6  
 RX: +0.75 DS DC X

Date: 28-05-1999  
 Time: 10:38  
 Age: 55

Fovea: OFF

RELIABILITY INDICES



SENSITIVITY PLOT

GREY-SCALE

3	-1	1	2				
0	-1	-2	-1	-1	-1		
-1	-1	-1	-2	-3	-1	-2	-1
-1	-1	-1	-1	-1	-1	-1	-1
-2	-1	-5	-3	-1	-1	0	-1
-2	-2	0	0	-1	-4	-2	-1
-3	-3	-2	1	-3	-3		
-2	-2	-1	-1				

3	-1	1	2				
1	-1	-1	-1	0	-1		
-1	-1	-1	-1	-3	-1	-1	-1
-1	-1	-1	-1	-1	0	-1	-1
-2	0	-4	-2	-1	-1	0	-1
-2	-2	0	0	-1	-3	-1	-1
-2	-2	-2	1	-3	-2		
-2	-1	-1	-1				

GHT  
 Within normal limits

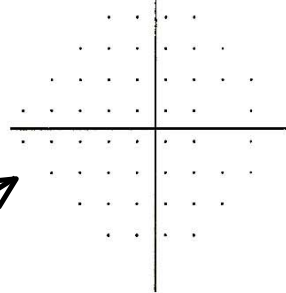
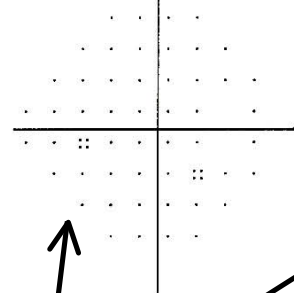
GLAUCOMA HEMIFIELD TEST

MD -1.45 dB  
 PSD 1.30 dB  
 SF 1.32 dB  
 CPSD 0.00 dB

GLOBAL INDICES

Total Deviation

Pattern Deviation



PROBABILITY PLOTS

- :: < 5%
- ⊗ < 2%
- ⊗ < 1%
- < 0.5%

EYE ASSOCIATES  
 DR IVAN GOLDBERG, DR GEOFFREY COHN  
 DR STUART GRAHAM, DR MARK GILLIES  
 187 MACQUARIE ST. SYDNEY

Figure 17. Print-out of the visual field from a right eye using a Humphrey Field Analyzer

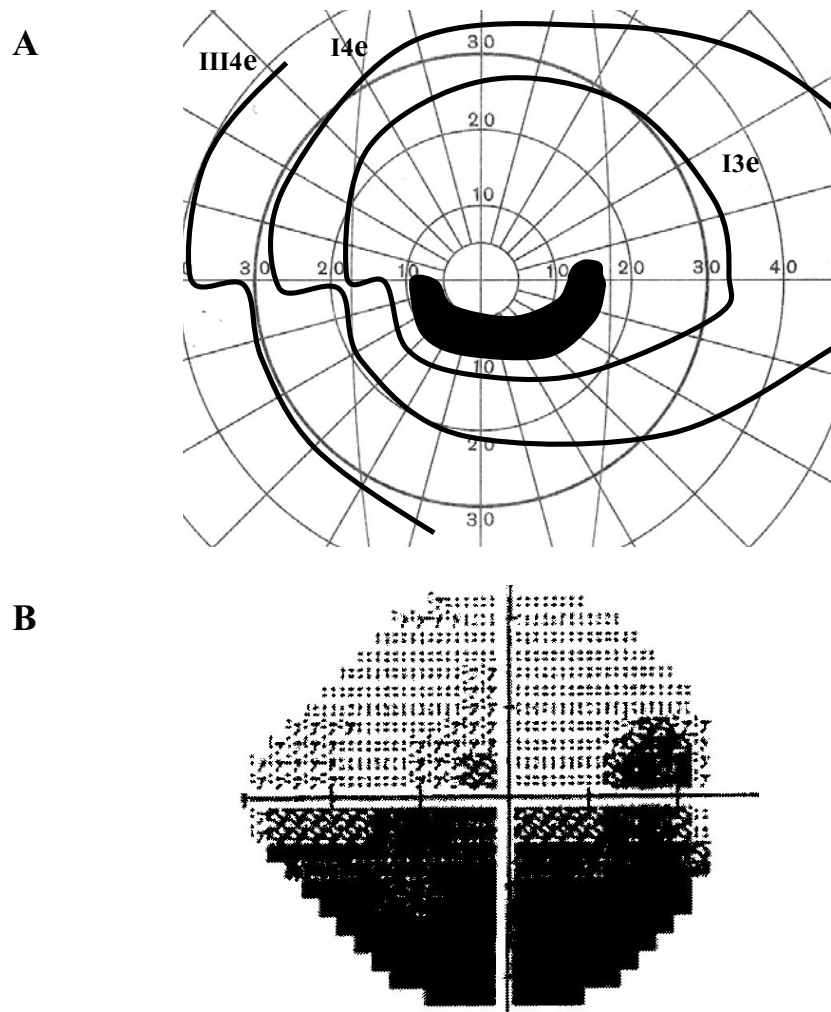


Figure 18. Visual field from the right eye using (A) manual kinetic perimetry and (B) automated static perimetry



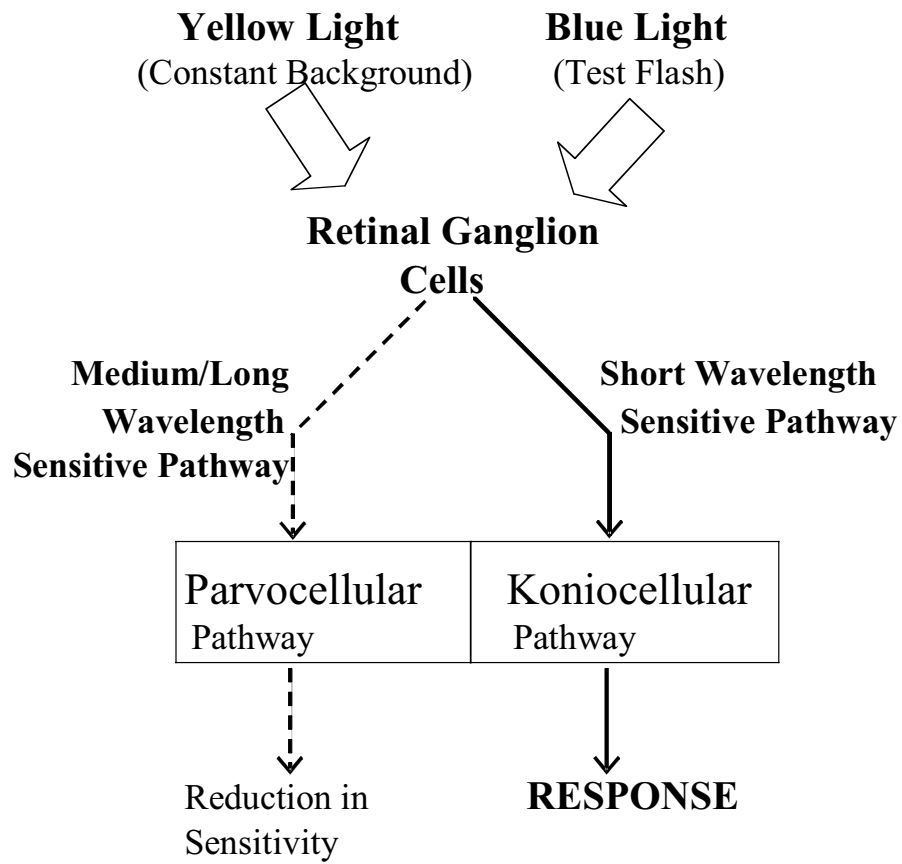


Figure 19. Schematic representation of the colour sensitive visual pathways

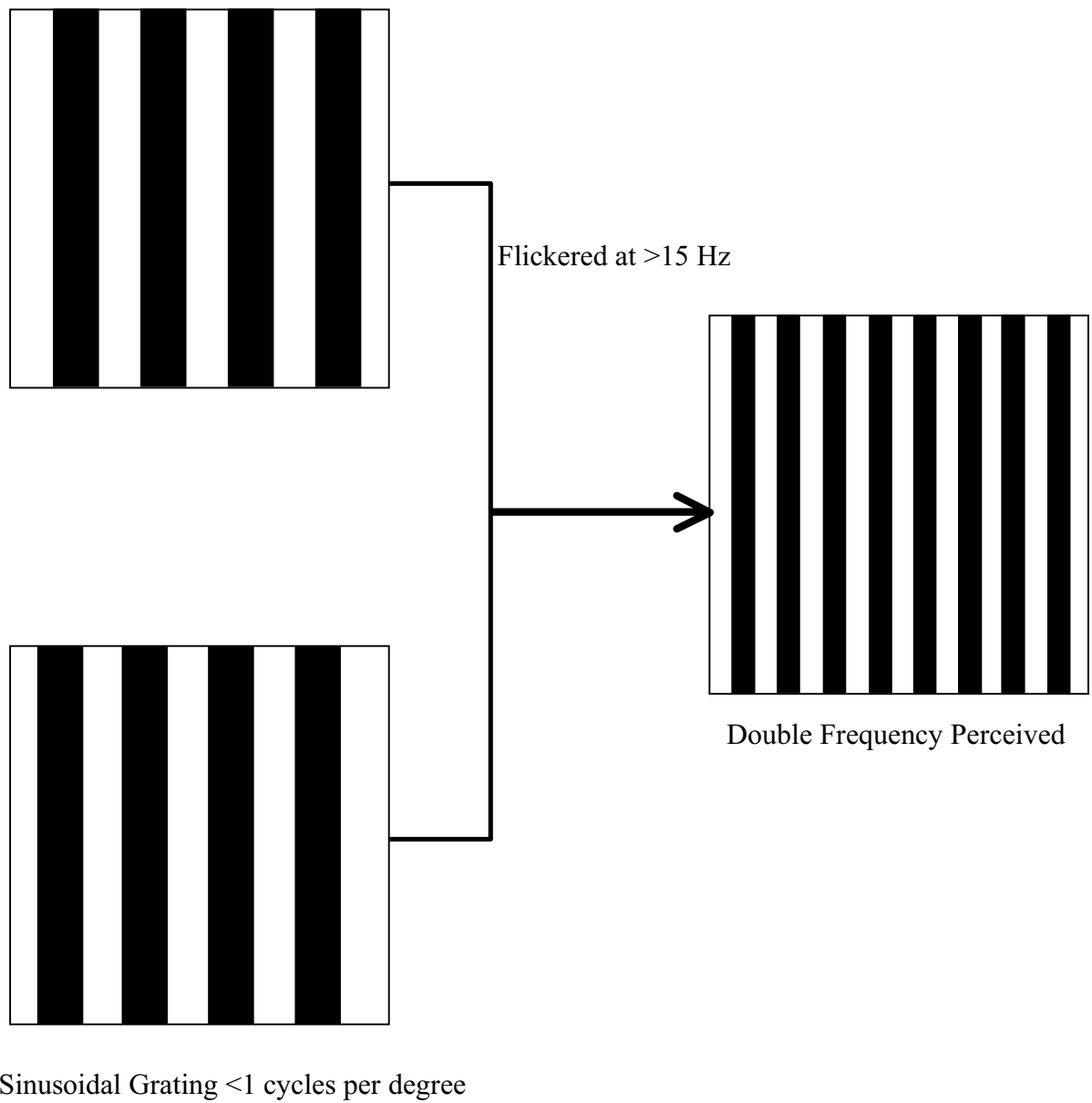


Figure 20. Schematic representation of the target used in frequency doubling perimetry



Figure 21. The Frequency Doubling Perimeter

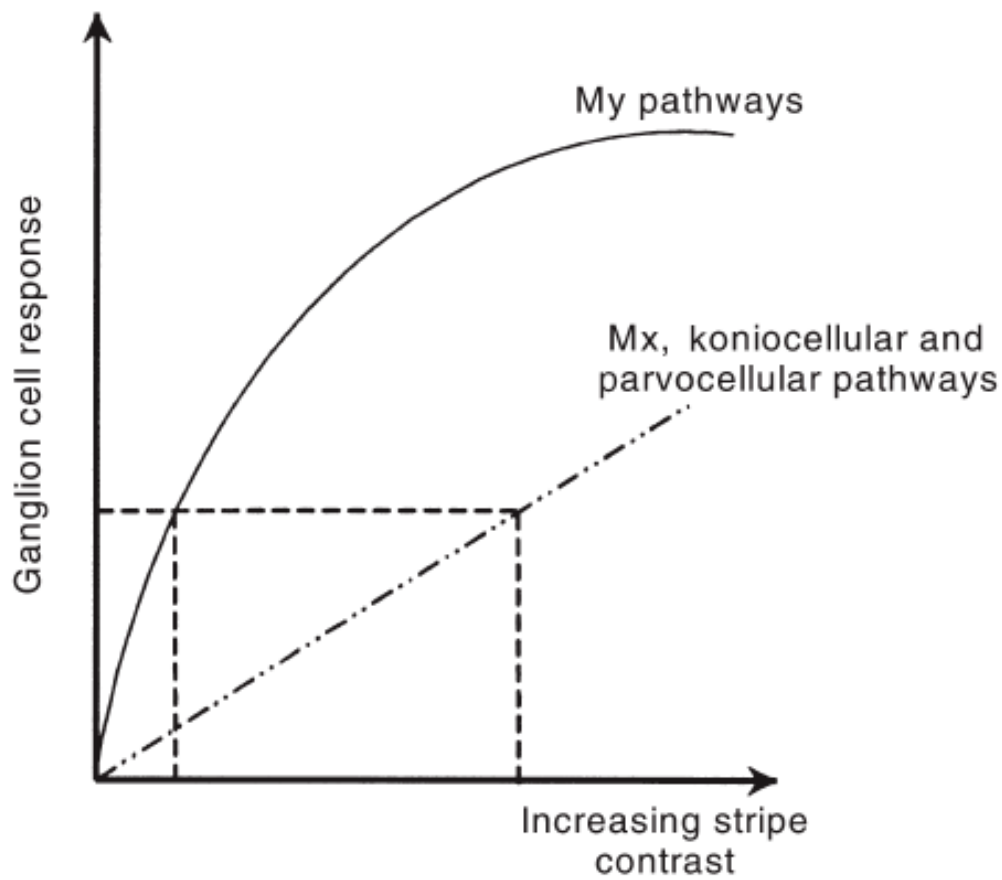


Figure 22. Relationship between change in target stripe contrast and My, Mx, Koniocellular and Parvocellular pathway responses (modified with permission from Prof. E Kaplan).<sup>217</sup> Shows the difference in target stripe contrast needed to achieve the same ganglion cell response.

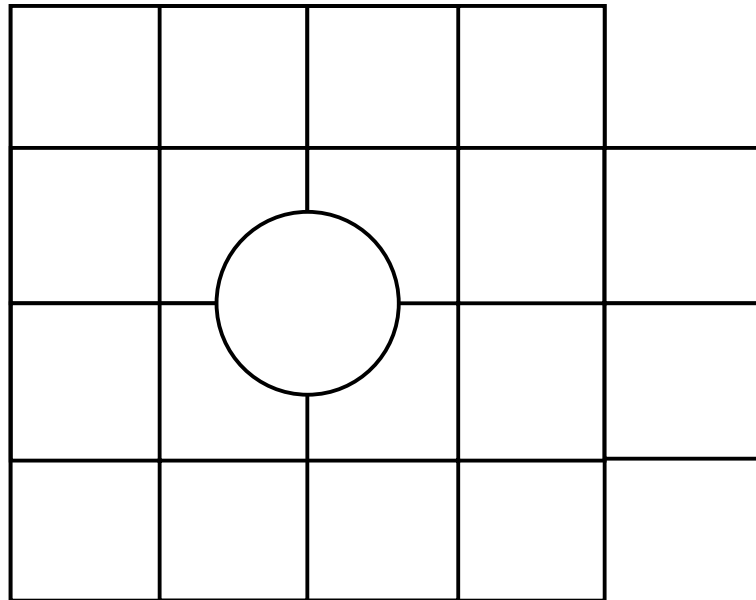
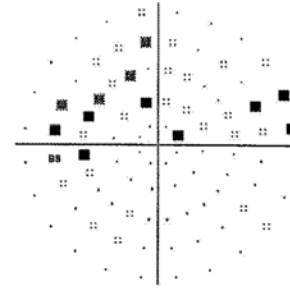
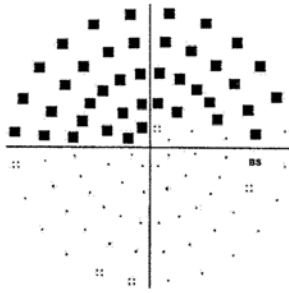


Figure 23. The testing pattern used by the frequency doubling perimeter to test the left eye

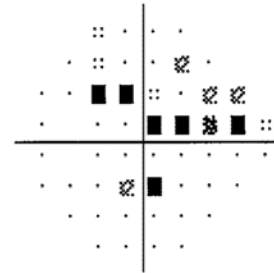
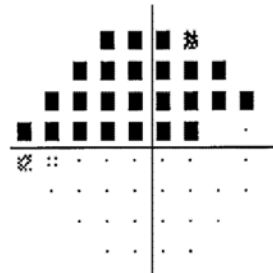
Patient

MF1

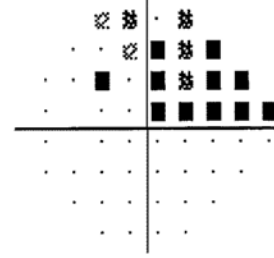
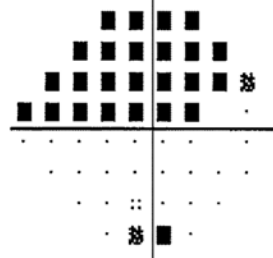
Medmont  
Central  
Threshold



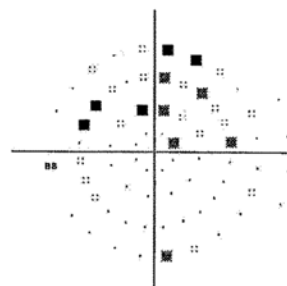
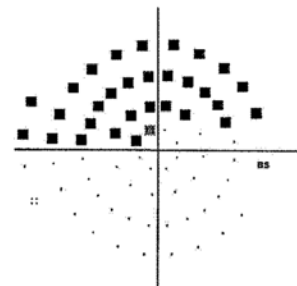
HFA  
Full  
Threshold



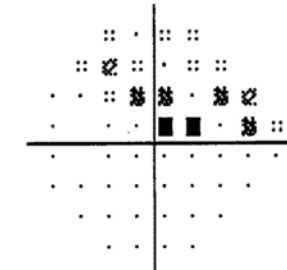
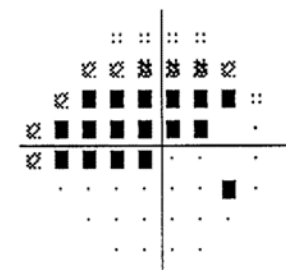
HFA  
SITA



Medmont  
Flicker



HFA  
Short  
Wavelength  
Automated  
Perimetry



Frequency  
Doubling  
Perimetry

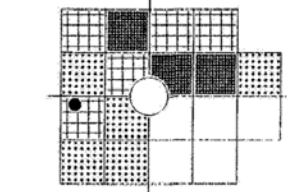
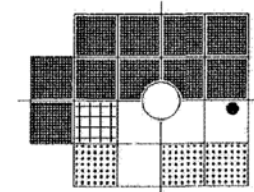


Figure 24. Pattern deviations from two patients (MF1, MF65).

Medmont probabilities: ::, < 6 dB; ■■, < 12 dB; ■, < 18 dB.

HFA probabilities: ::, P < 5%; ■■, P < 2%; ■■, P < 1%; ■, P < 0.5%.

FDP probabilities: ■■■■, P < 5%; ■■■, P < 1%; ■■■, P < 0.5%

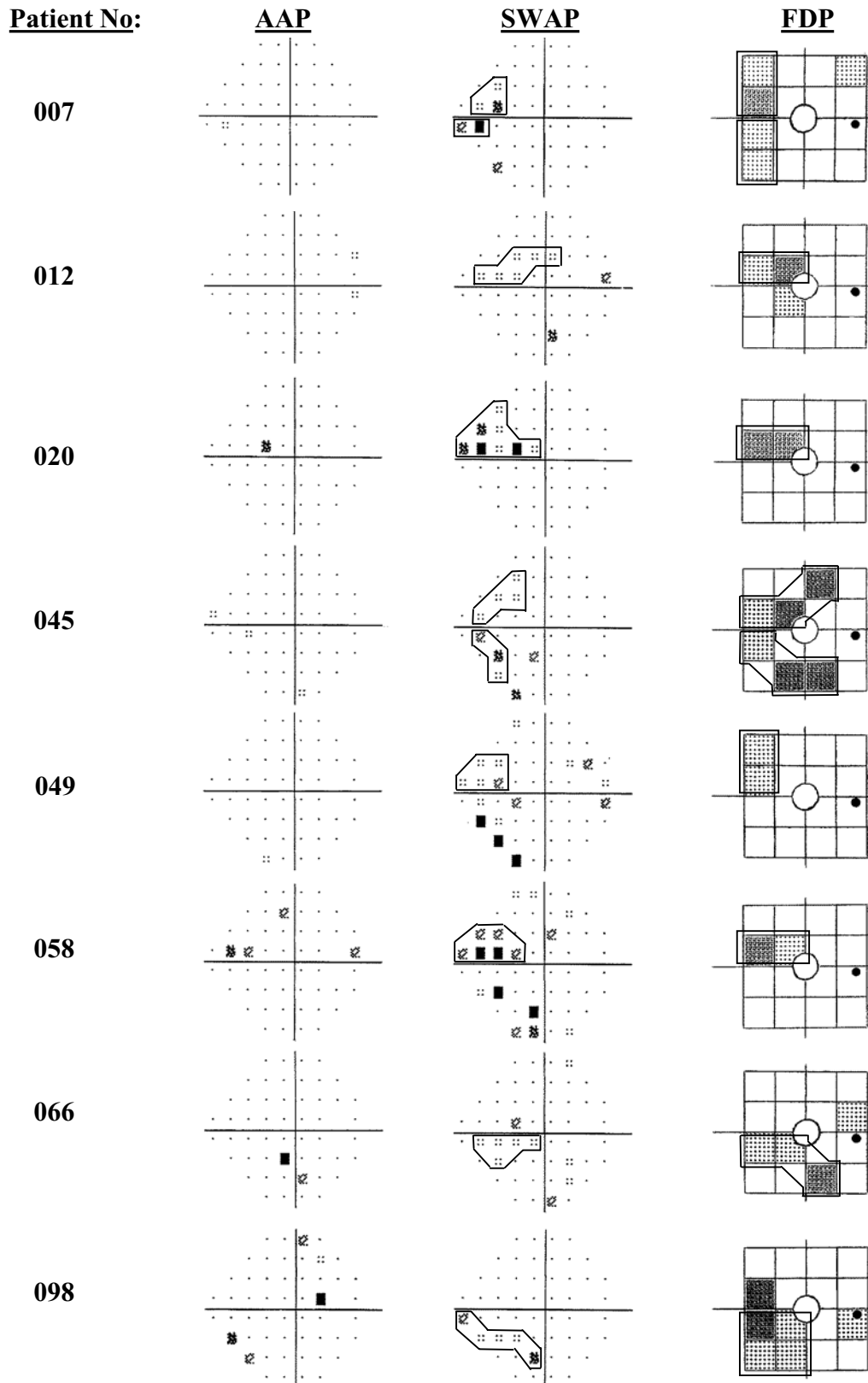


Figure 25. Pattern deviations from those patients both with short wavelength automated perimetry (SWAP) and frequency doubling perimetry (FDP) losses. Achromatic automated perimetry (AAP) and SWAP probabilities:  $\ddot{\cdot}$ ,  $P < 5\%$ ;  $\otimes$ ,  $P < 2\%$ ;  $\otimes$ ,  $P < 1\%$ ;  $\blacksquare$ ,  $P < 0.5\%$ . FDP probabilities:  $\text{grid}$ ,  $P < 5\%$ ;  $\text{grid}$ ,  $P < 1\%$ . Areas of visual field loss are outlined.

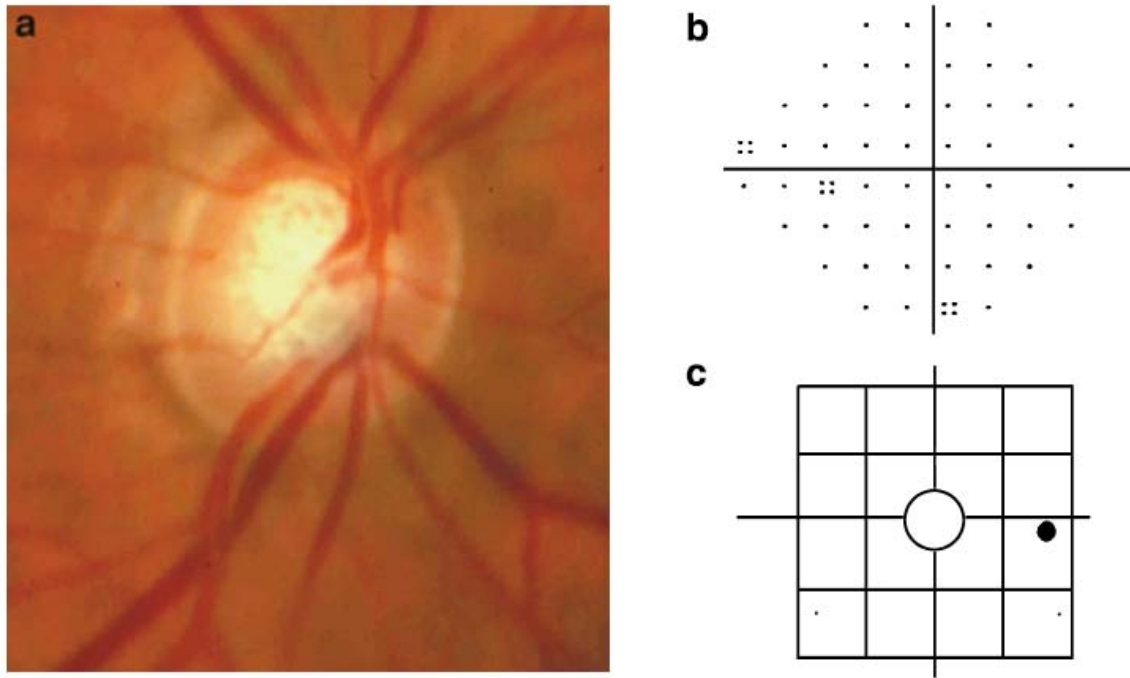


Figure 26. (a) Disc photograph; (b) short wavelength automated perimetry visual field; and (c) frequency doubling perimetry visual field from a false negative subject.



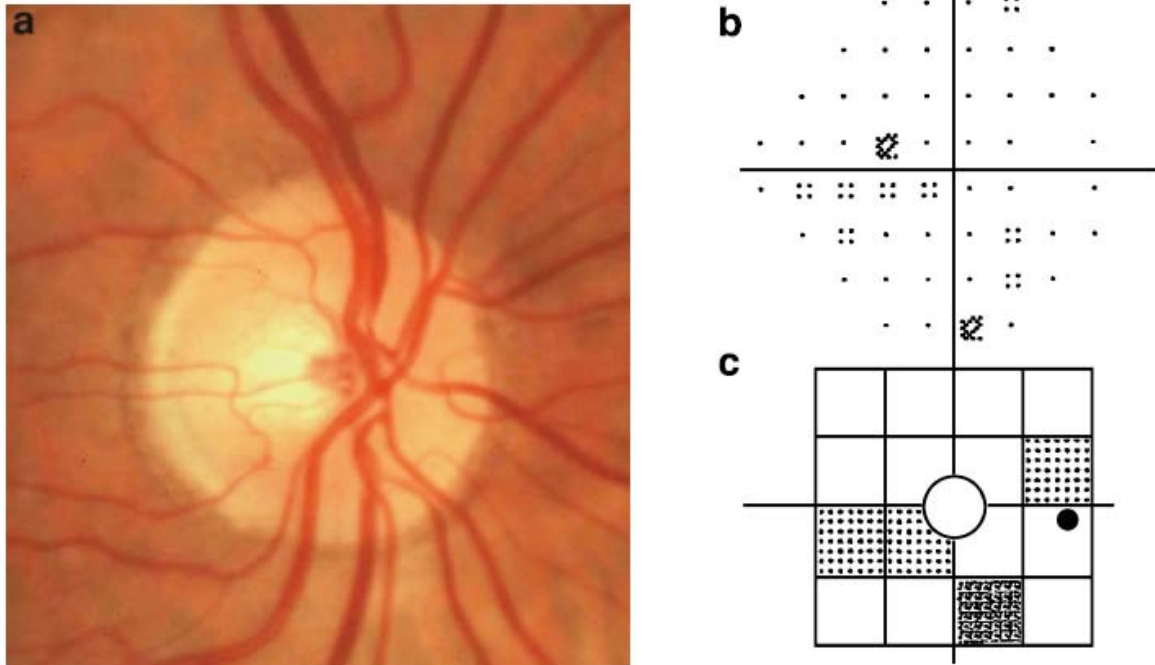


Figure 27. (a) Disc photograph; (b) short wavelength automated perimetry visual field; and (c) frequency doubling perimetry visual field from a false positive subject.

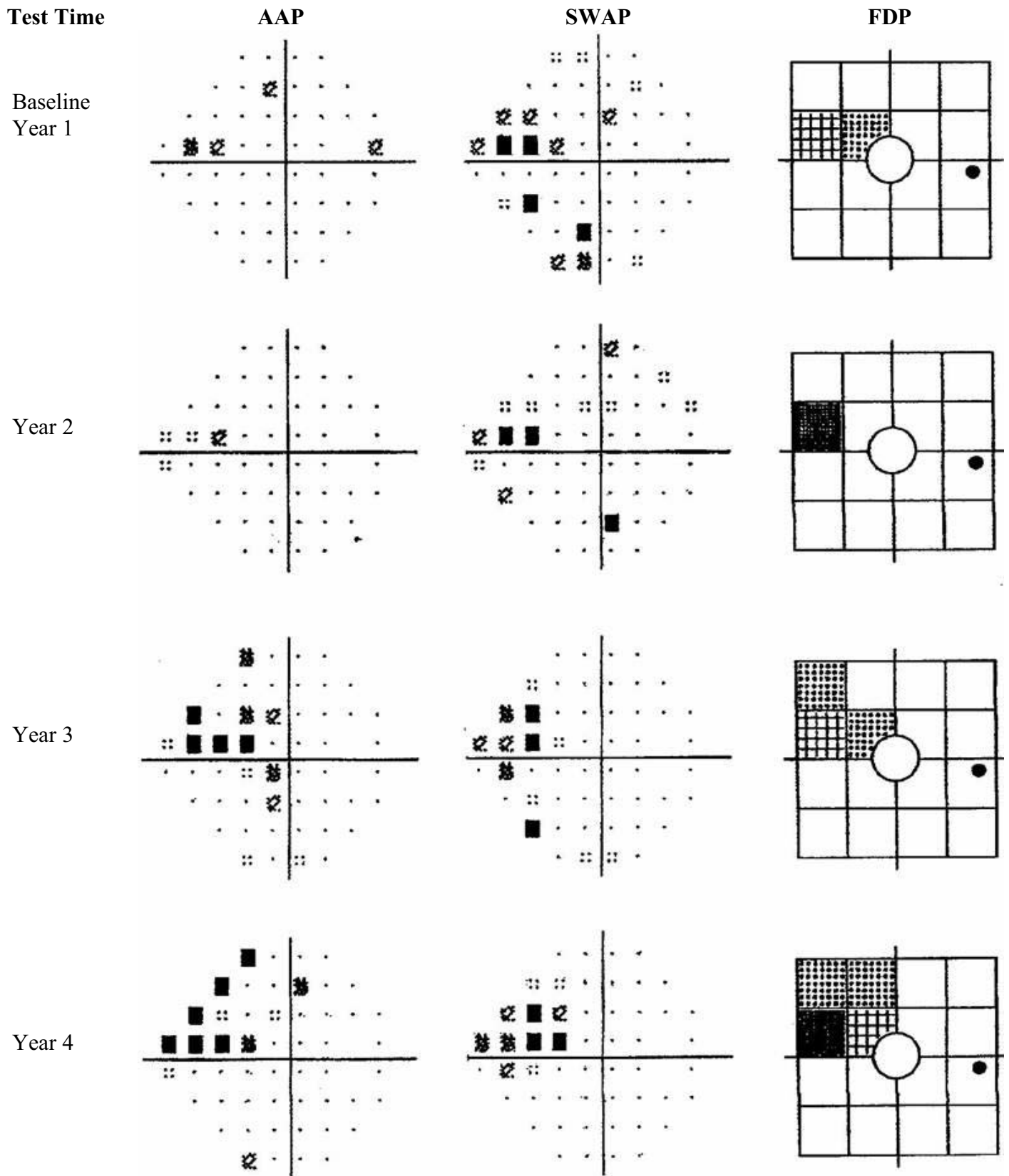


Figure 28. Pattern deviations from Patient 058 for Achromatic Automated Perimetry (AAP), Short Wavelength Automated Perimetry (SWAP) and Frequency Doubling Perimetry (FDP) over the four year study period.

HFA probabilities:  $\ddot{\cdot}$ ,  $P < 5\%$ ;  $\otimes$ ,  $P < 2\%$ ;  $\otimes$ ,  $P < 1\%$ ;  $\blacksquare$ ,  $P < 0.5\%$ .

FDP probabilities:  $\text{grid}$ ,  $P < 5\%$ ;  $\text{grid}$ ,  $P < 1\%$ ;  $\text{grid}$ ,  $P < 0.5\%$

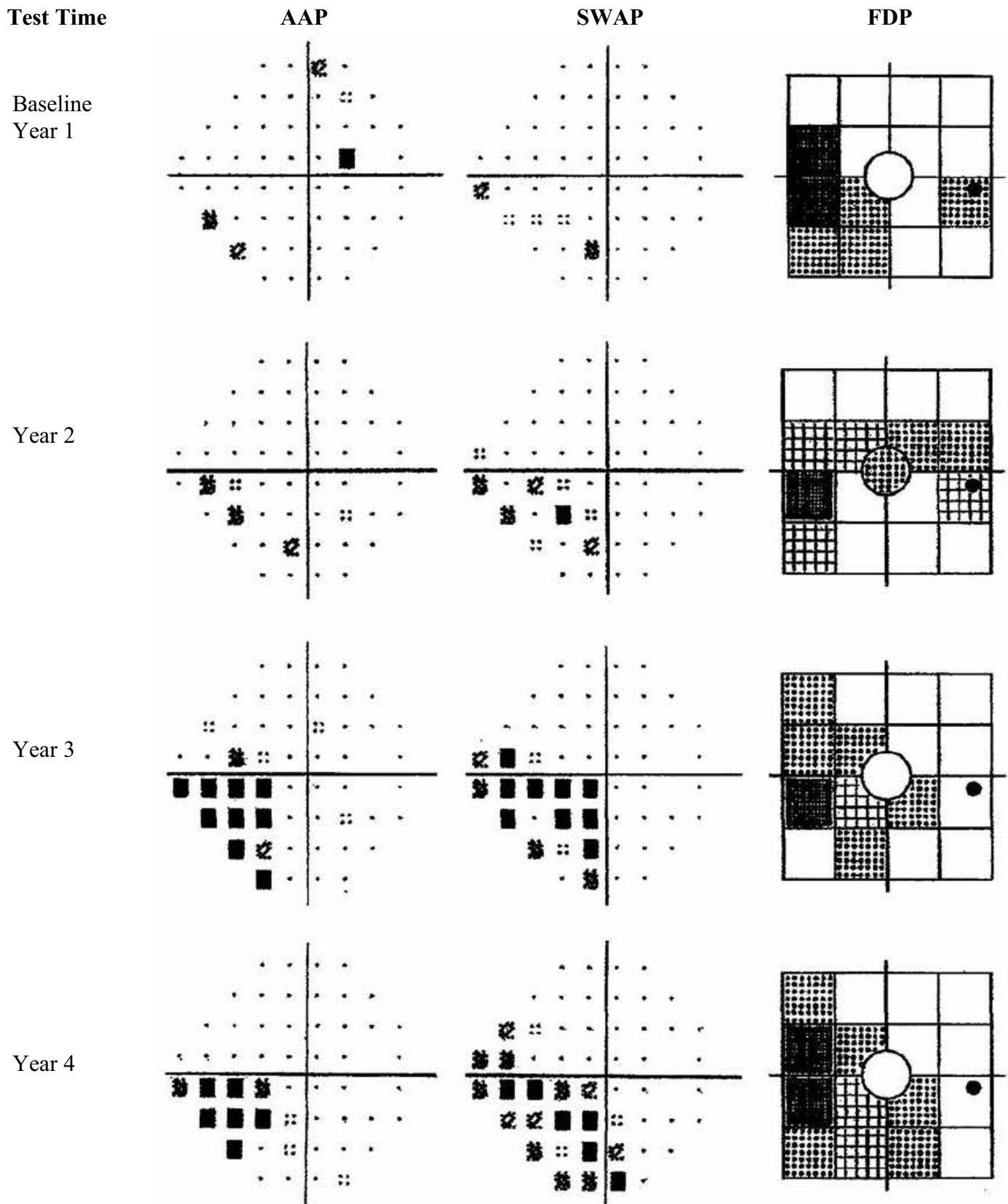


Figure 29. Pattern deviations from Patient 098 for Achromatic Automated Perimetry (AAP), Short Wavelength Automated Perimetry (SWAP) and Frequency Doubling Perimetry (FDP) over the four year study period.

HFA probabilities:  $\ddot{\cdot}$ ,  $P < 5\%$ ;  $\otimes$ ,  $P < 2\%$ ;  $\text{⊞}$ ,  $P < 1\%$ ;  $\blacksquare$ ,  $P < 0.5\%$ .

FDP probabilities:  $\text{⊞}$ ,  $P < 5\%$ ;  $\text{⊞}$ ,  $P < 1\%$ ;  $\blacksquare$ ,  $P < 0.5\%$

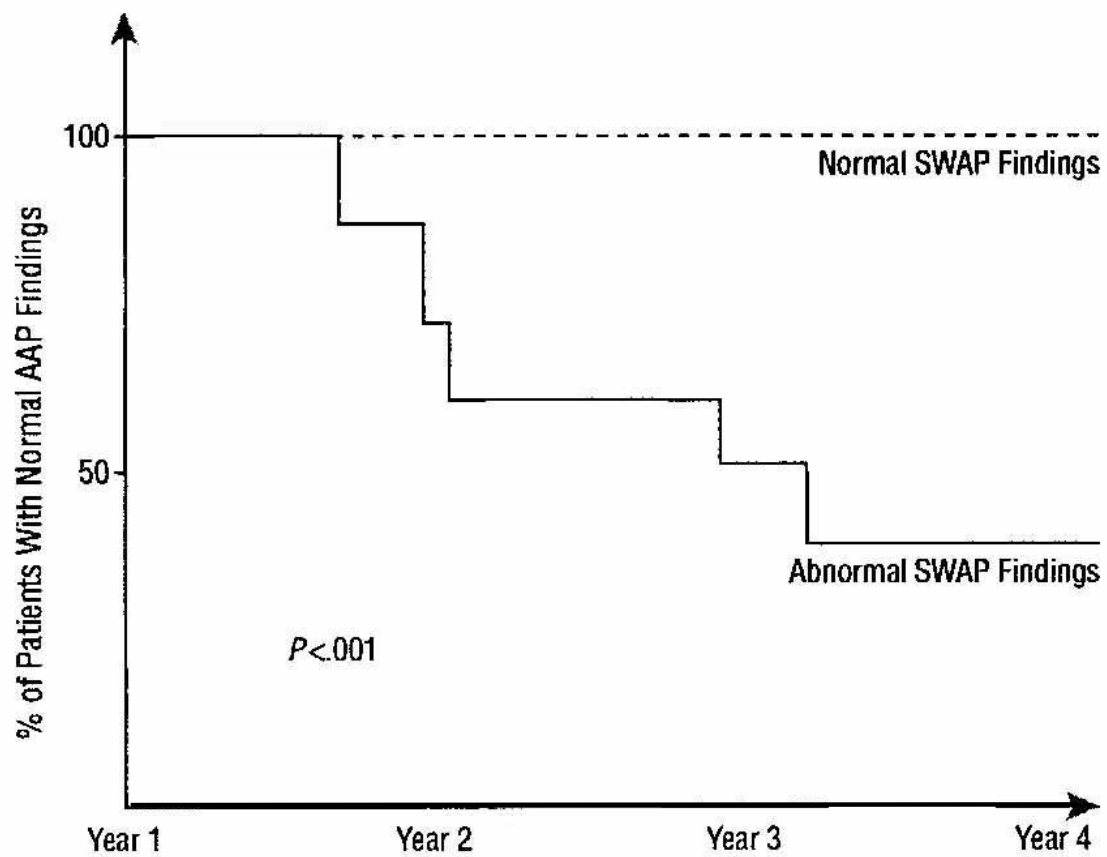


Figure 30. Survival curve of patients with normal SWAP and abnormal SWAP, using the development of an AAP abnormality as end point.

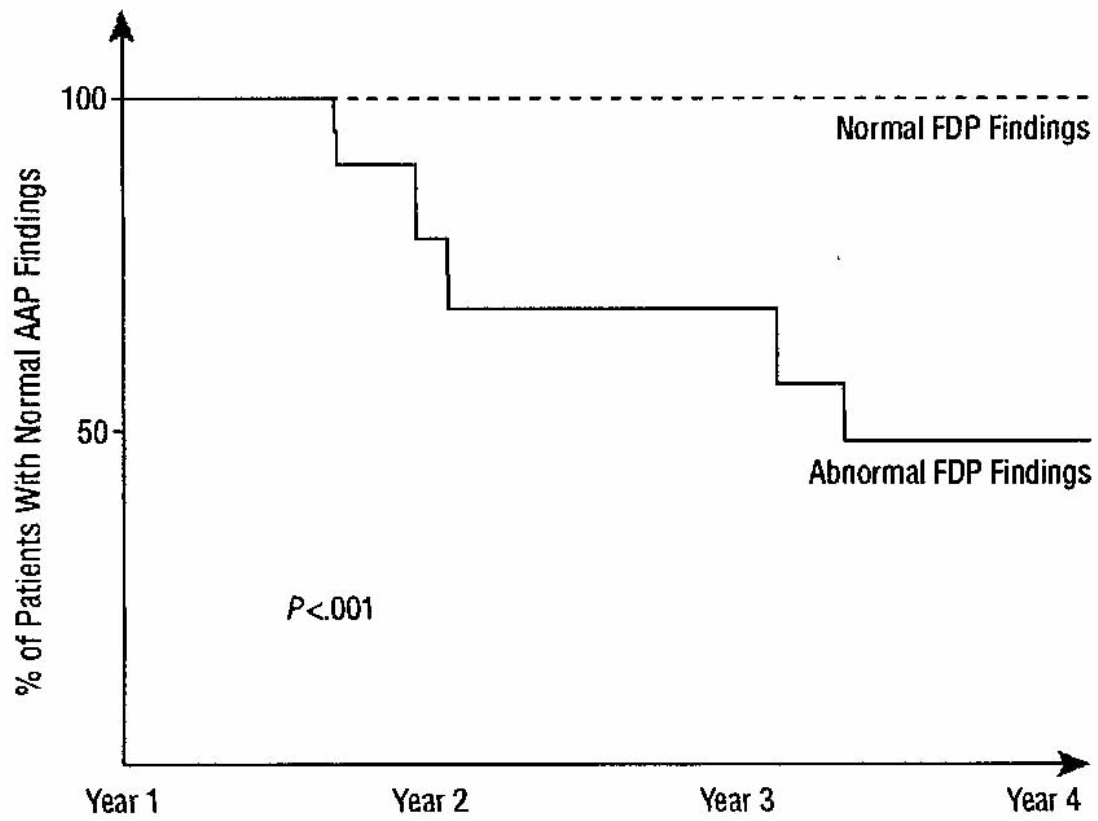


Figure 31. Survival curve patients with normal FDP and abnormal FDP, using the development of an AAP abnormality as end point.

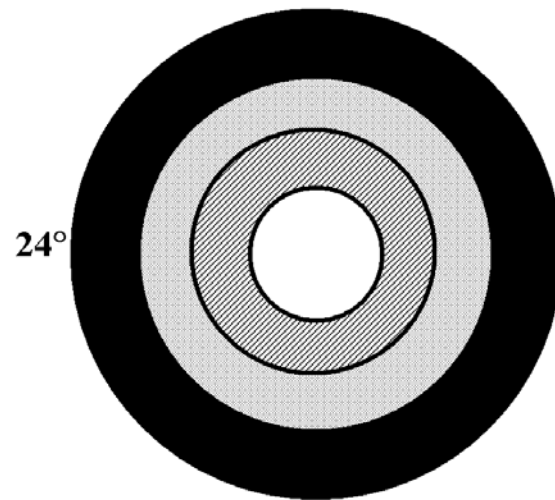
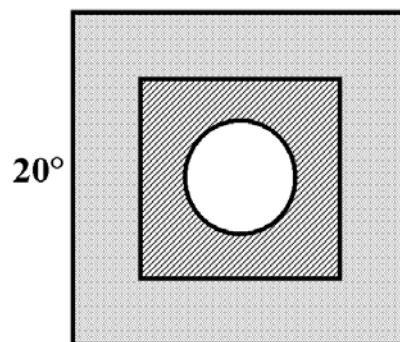
**A.****B.**

Figure 32. The position of visual fields zones for: **A.** Humphrey Field Analyzer for AAP and SWAP and **B.** Frequency Doubling Perimeter.

(□ Zone 1 (10° eccentricity), ▨ Zone 2 (15° eccentricity),

■ Zone 3 (20° eccentricity), ■ Zone 4 (24° eccentricity))

(Eccentricity of the visual field is indicated)

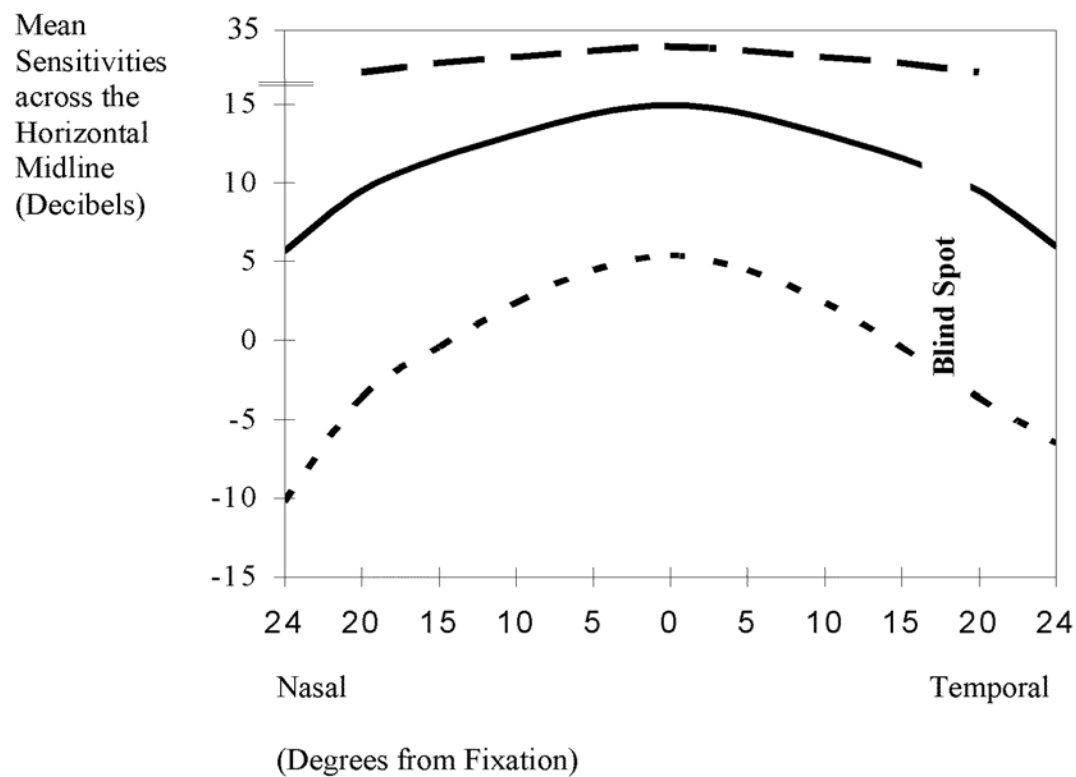


Figure 33. Graph of Mean Sensitivities across the Horizontal Midline of the Visual Field for: — Achromatic Automated Perimetry, ..... Short Wavelength Automated Perimetry and - - - Frequency Doubling Perimetry.

(N.B Mean Sensitivities for Achromatic Automated Perimetry and Short Wavelength Automated Perimetry have been converted to Contrast Decibels in order to be Comparable with Frequency Doubling Perimetry)

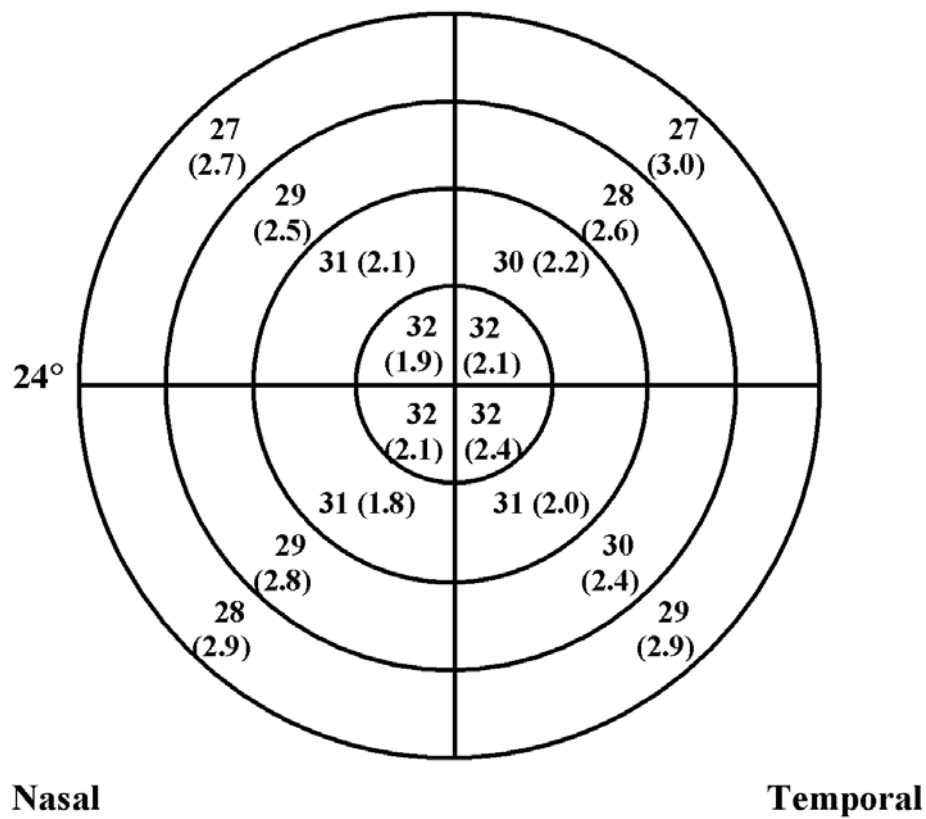


Figure 34. Mean Visual Field Sensitivities in Decibels (Standard Deviation) for each Quadrant of each Zone for Achromatic Automated Perimetry using the Humphrey Field Analyzer.  
(Eccentricity of the visual field is indicated)



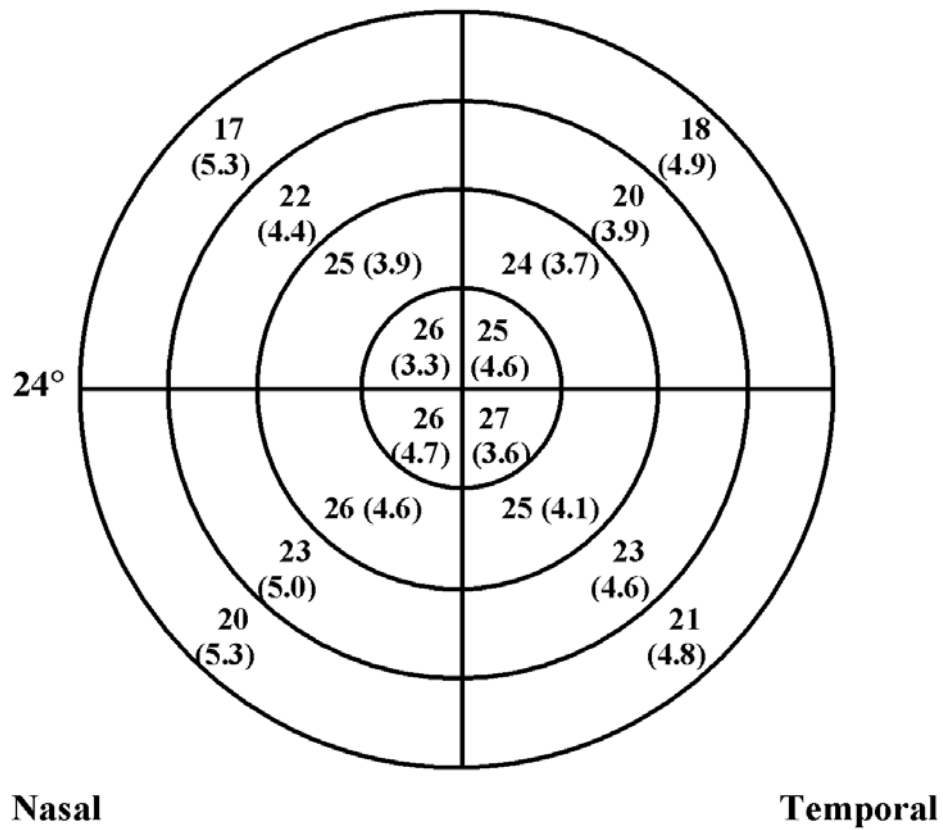


Figure 35. Mean Visual Field Sensitivities in Decibels (Standard Deviation) for each Quadrant of each Zone for Short Wavelength Automated Perimetry using the Humphrey Field Analyzer.  
(Eccentricity of the visual field is indicated)

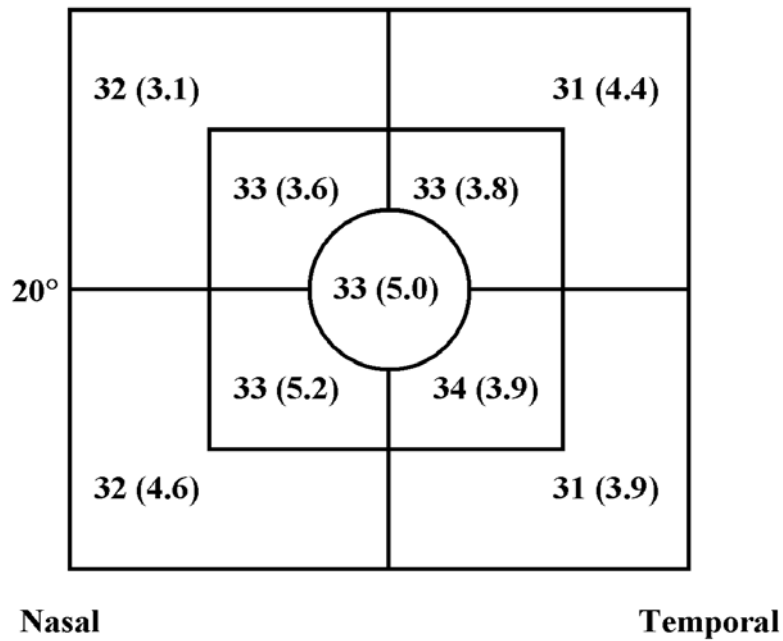


Figure 36. Mean Visual Field Sensitivities in Decibels (Standard Deviation) for each Quadrant of each Zone for the Frequency Doubling Perimeter. (Eccentricity of the visual field is indicated)

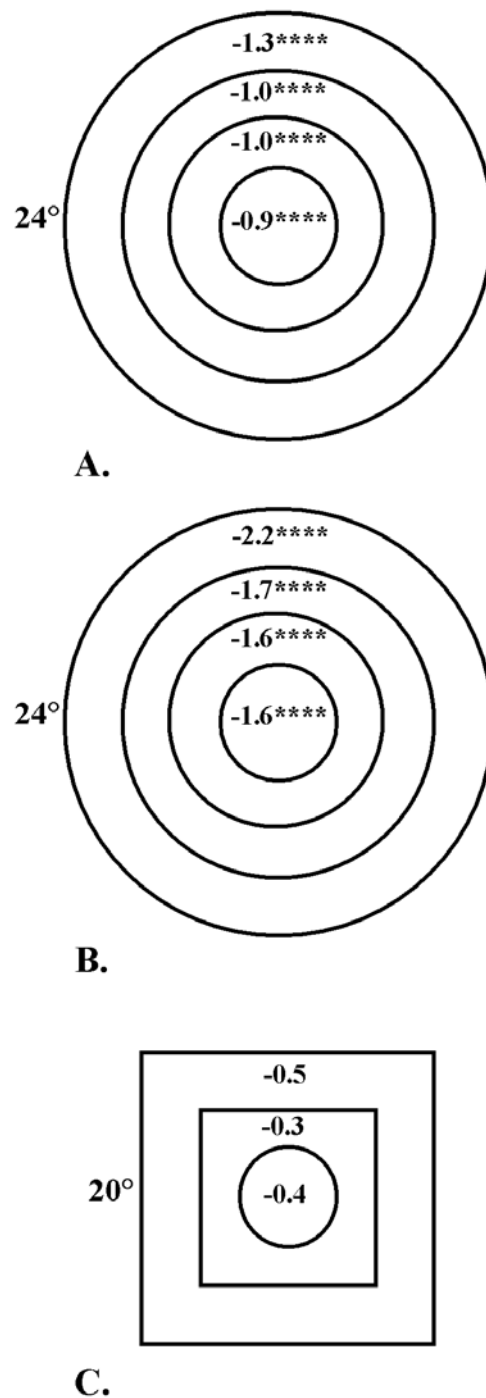


Figure 37. The Slope of the Regression of Mean Sensitivity (Decibels) at each Visual Field Zone as a function of Decade of Age for **A.** Achromatic Automated Perimetry, **B.** Short Wavelength Automated Perimetry and **C.** Frequency Doubling Perimetry.

(\* P<0.05, \*\* P<0.01, \*\*\*P<0.001, \*\*\*\*P<0.0001)

(Eccentricity of the visual field is indicated)

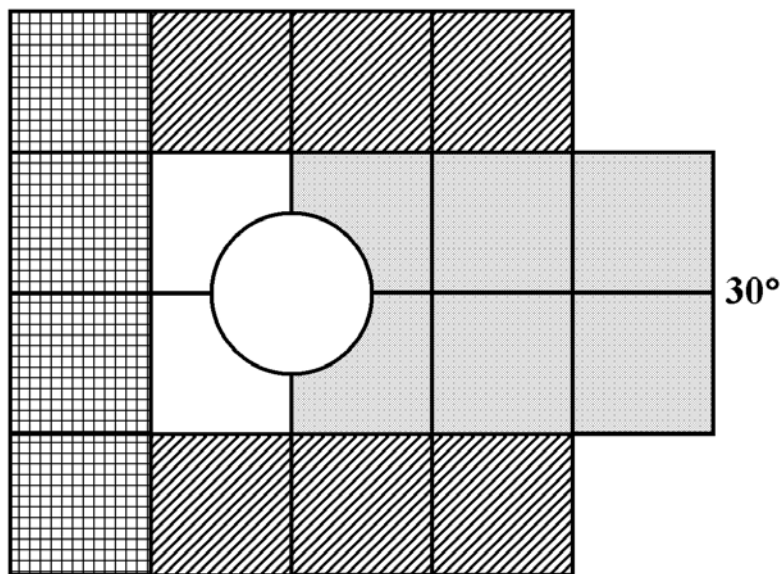





Figure 38. Showing the Area Contributing to a Nasal Step location,  an Arcuate location,  and a Temporal Wedge  Above and Below the Horizontal Midline in the Left Visual Field.

(Eccentricity of the visual field is indicated)

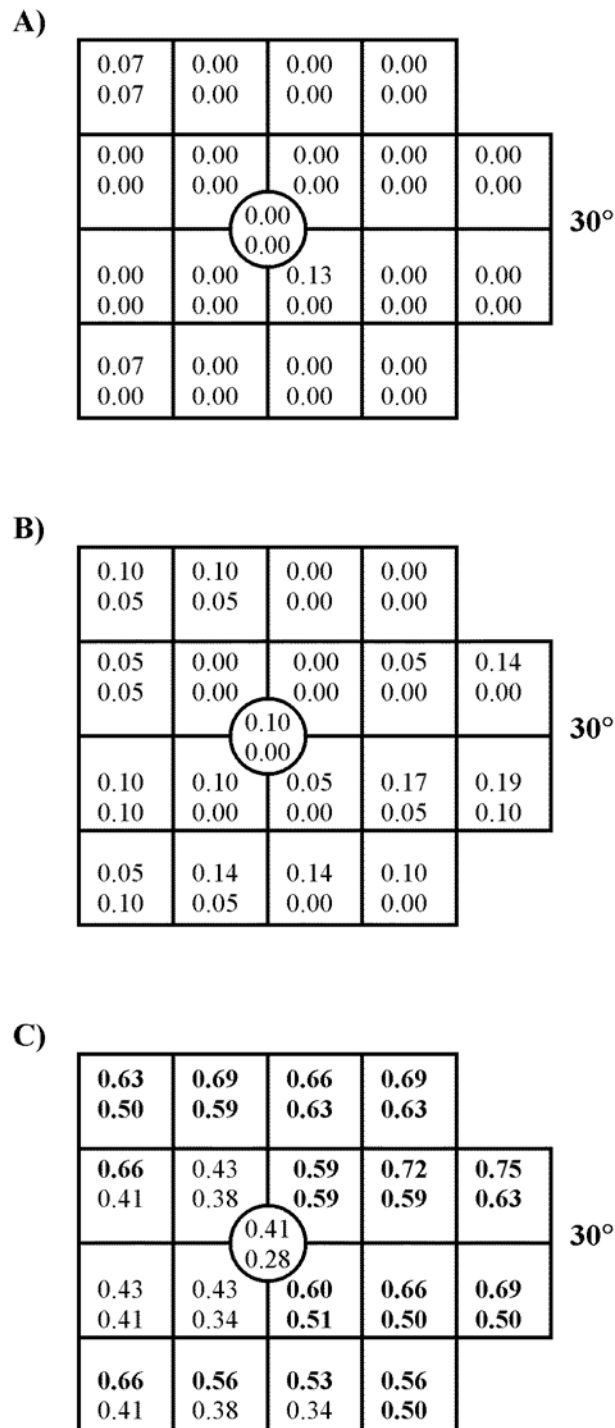


Figure 39. Showing Frequencies of Abnormal Zones for A) Controls, B) Glaucoma Suspects and C) Open-Angle Glaucoma Patients in the Left Visual Field.

(P<5%; upper frequency, P<1%; lower frequency)

(Frequencies ≥ 0.50 are Highlighted)

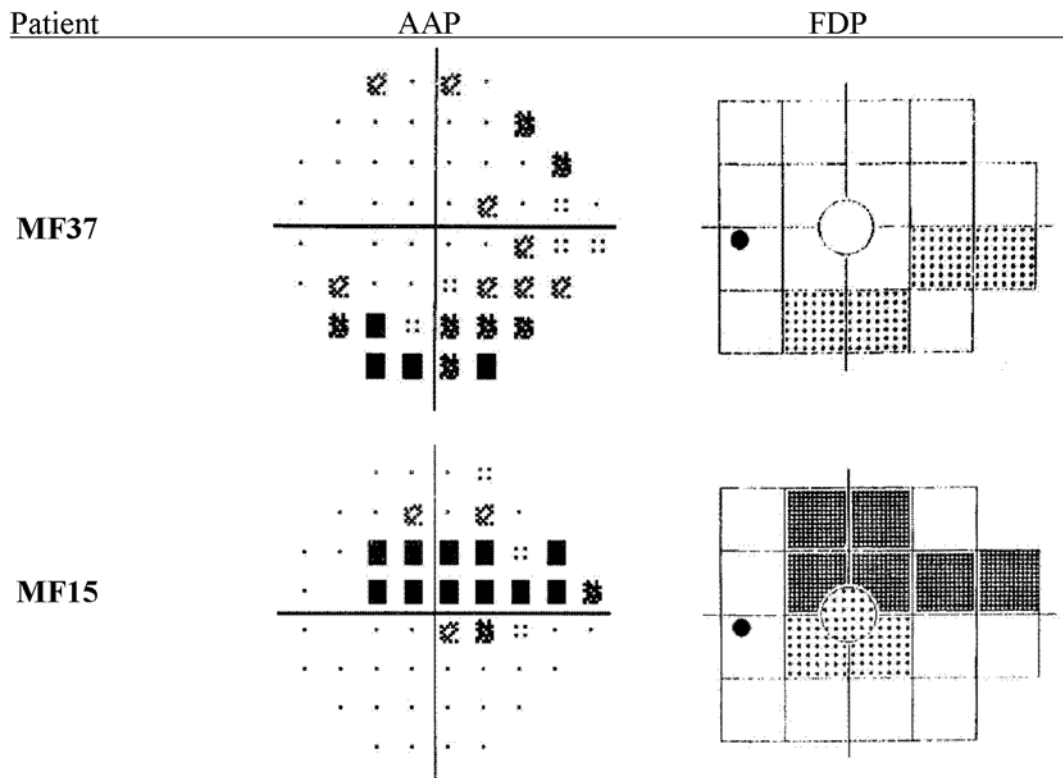


Figure 40a. Showing Pattern Deviations from Patients Classified by Frequency Doubling Perimetry as True Positives Under a Nasal-Step Protocol.

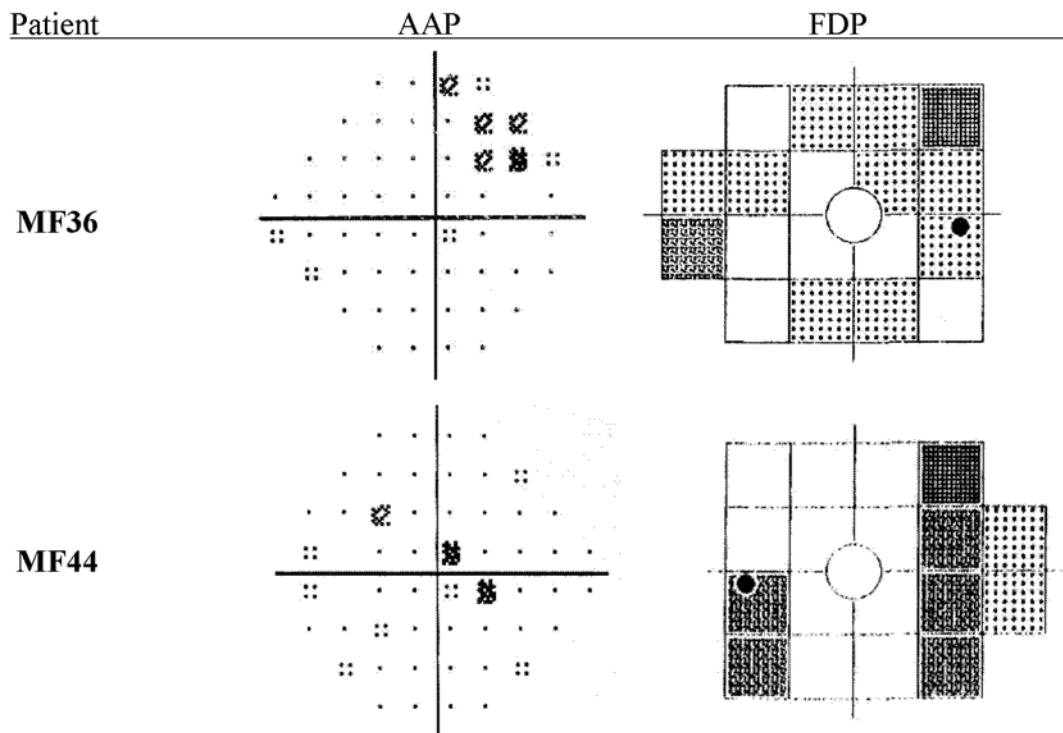


Figure 40b. Showing Pattern Deviations from Patients Classified by Frequency Doubling Perimetry as False Positives Under a Nasal-Step Protocol.

(AAP Probabilities: ∴, P < 5%; ⊗, P < 2%; ⊞, P < 1%; ■, P < 0.5%)

(FDP Probabilities: ▤ P < 5%, ▨ P < 1%, ▩ P < 0.5%)

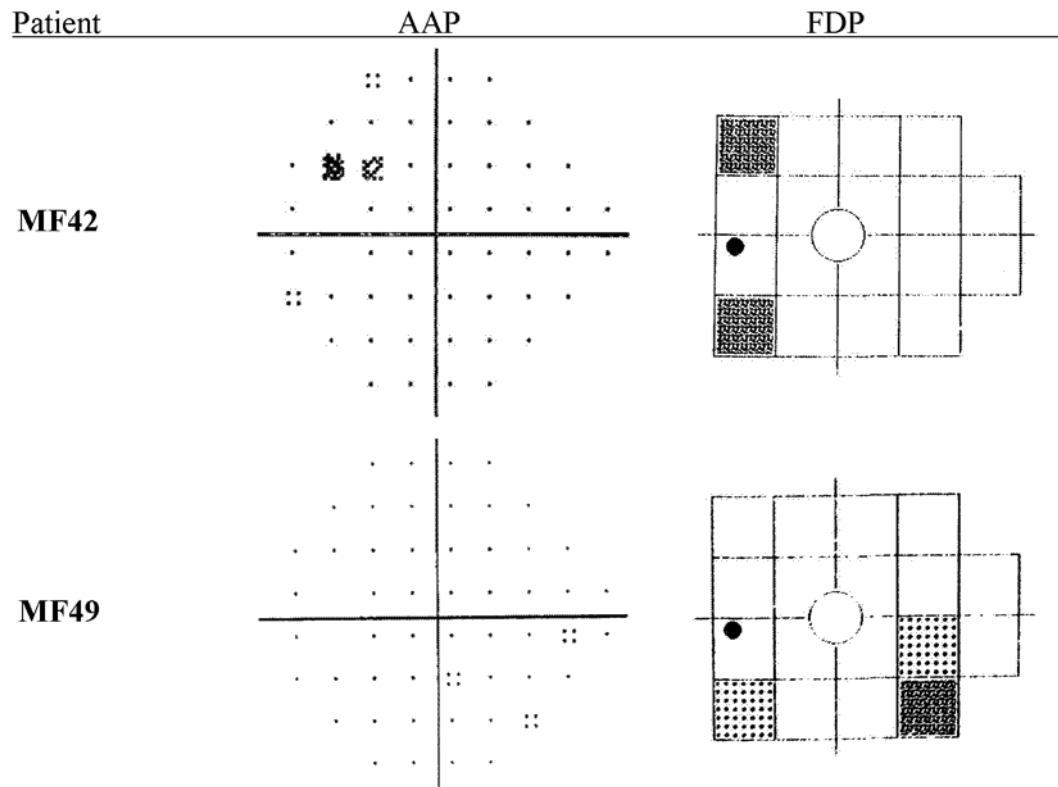


Figure 41a. Showing Pattern Deviations from Patients Classified by Frequency Doubling Perimetry as True Negatives Under a Nasal-Step Protocol.

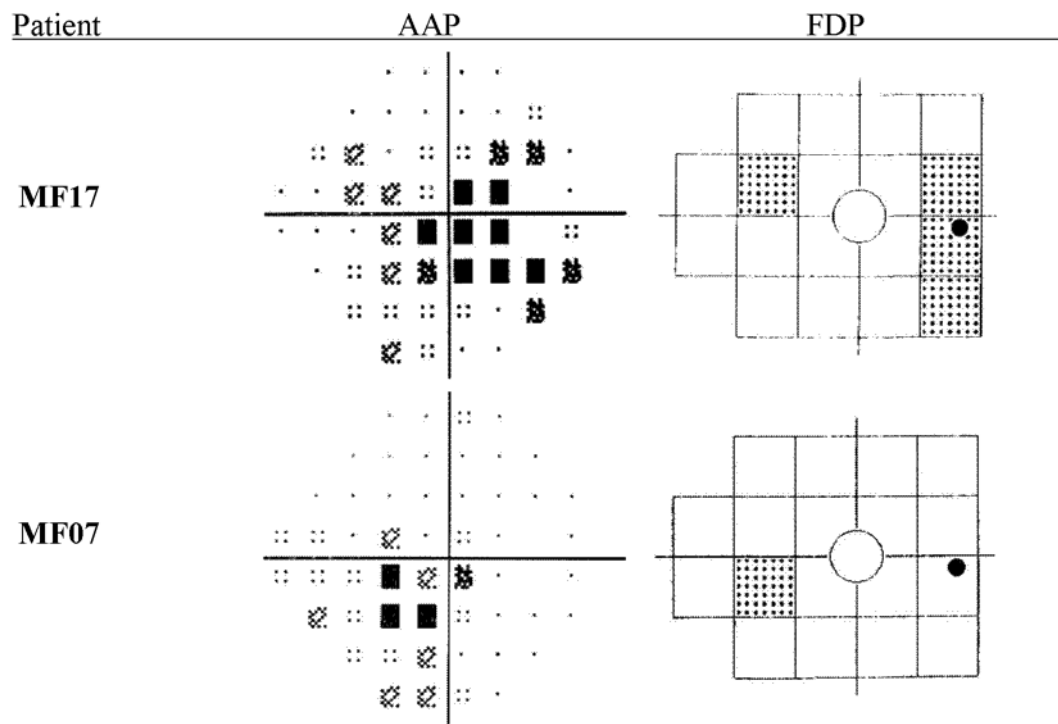


Figure 41b. Showing Pattern Deviations from Patients Classified by Frequency Doubling Perimetry as False Negatives Under a Nasal-Step Protocol.

(AAP Probabilities: ::, P < 5%; ☒, P < 2%; ☒, P < 1%; ■, P < 0.5%)

(FDP Probabilities: ☒ P < 5%, ☒ P < 1%, ☒ P < 0.5%)



Figure 42. The Humphrey Matrix perimeter



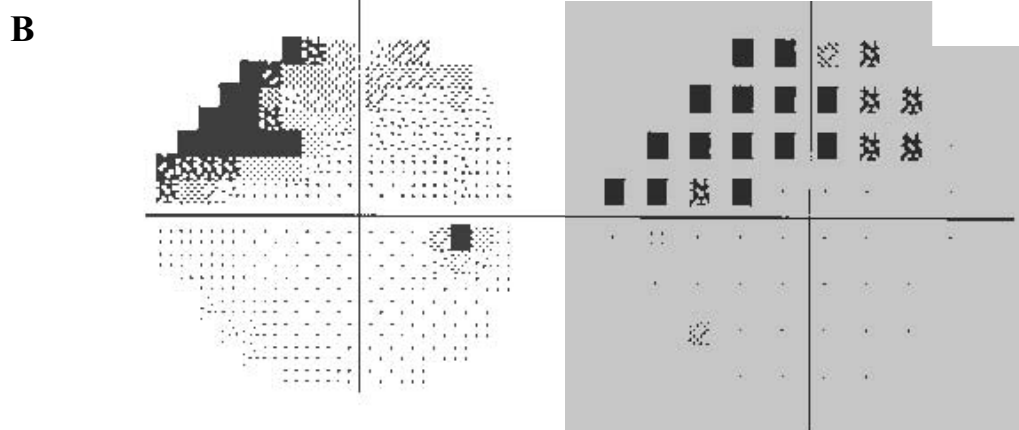
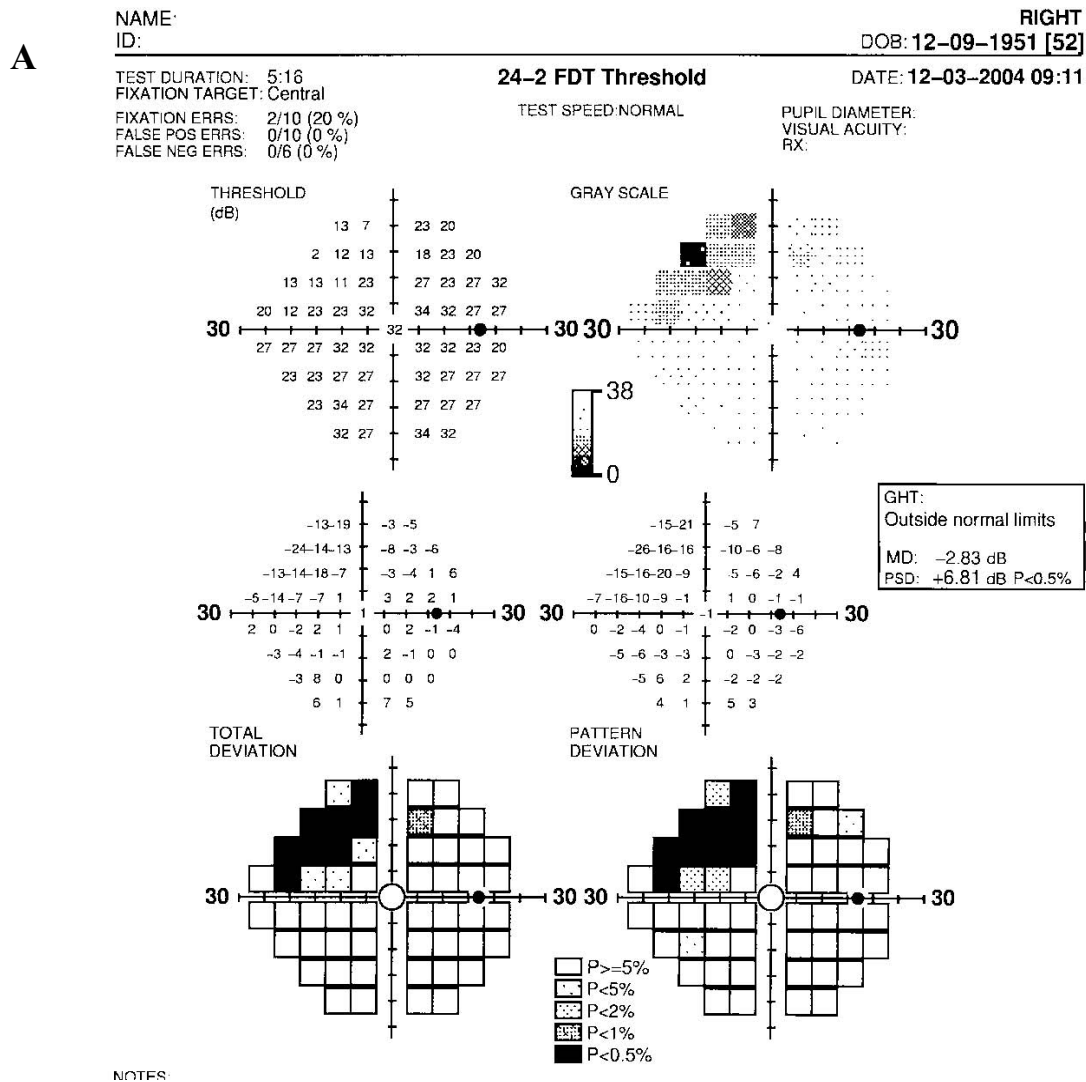


Figure 43. The print-out from (A) the Humphrey Matrix perimeter, compared with (B) the Humphrey Field Analyzer

---

Short Wavelength Automated Perimetry			
	Abnormal	Normal	TOTAL
<hr/>			
Frequency Doubling Perimetry			
Abnormal	8	2	10
Normal	1	51	52
TOTAL	9	53	62

---

Table 1. Numbers of Normal and Abnormal Frequency Doubling Perimetry and Short Wavelength Automated Perimetry in the patient sample.

FDP result	SWAP result		Total
	Abnormal	Normal	
Abnormal	3	0	3
Normal	1	8	9
Total	4	8	12

Table 2. Results of short wavelength automated perimetry (SWAP) compared with frequency doubling perimetry (FDP) for patients with an abnormal clinical optic disc assessment.

---

FDP result	SWAP result		
	Abnormal	Normal	Total
Abnormal	3	1	4
Normal	0	34	34
Total	3	35	38

---

Table 3. Results of short wavelength automated perimetry (SWAP) compared with frequency doubling perimetry (FDP) for patients with a normal clinical optic disc assessment.

---

SWAP result	Clinical optic disc assessment		
	Abnormal	Normal	Total
Abnormal	4	3	7
Normal	8	35	43
Total	12	38	50

---

Table 4. Results of short wavelength automated perimetry (SWAP) compared with clinical optic disc assessment.

---

SWAP result	Clinical optic disc assessment		
	Abnormal	Normal	Total
Abnormal	3	4	7
Normal	9	34	43
Total	12	38	50

---

Table 5. Results of frequency doubling perimetry (FDP) compared with clinical optic disc assessment.

---

—

Group	Number	Males (%)	Mean age (SD)	Range
Control	15	7 (47%)	52 years (15 years)	29–75 years
Glaucoma suspects	8	5 (63%)	56 years (16 years)	35–77 years
Ocular hypertension	8	1 (13%)	60 years (9 years)	47–74 years
Open angle glaucoma	32	16 (50%)	64 years (9 years)	41–79 years

---

Table 6 Description of patients within the study groups

Humphrey			
Full Threshold MD			
Group	Average	(SD)	Range
Control	- 0.75	(1.05)	0.59 to -2.34
Glaucoma Suspects	- 0.66	(1.23)	1.57 to -1.72
Ocular Hypertension	- 1.19	(2.39)	0.90 to -6.41
Open Angle Glaucoma	- 8.20	(7.51)	1.04 to -26.58

Table 7. Description the amount of visual field loss for patients within the study groups



	Mean Test Time	Standard Deviation
Medmont Central Threshold	10 minutes 51 seconds	51 seconds
Medmont Flicker Perimetry	9 minutes 47 seconds	1 minutes 6 seconds
Humphrey Full Threshold	10 minutes 43 seconds	1 minutes 26 seconds
Humphrey SITA	5 minutes 44 seconds	1 minutes 12 seconds
Short Wavelength Automated Perimetry	10 minutes 35 seconds	1 minutes 43 seconds
Frequency Doubling Perimetry	5 minutes 8 seconds	30 seconds

Table 8. Mean test time (standard deviation) for Humphrey and Medmont perimetry

	Humphrey Full Threshold		Humphrey SITA	
	Abnormal	Normal	Abnormal	Normal
<hr/>				
Medmont Central Threshold (Strict)				
Abnormal	24	2	25	1
Normal	1	36	2	35
<hr/>				
Medmont Central Threshold (Loose)				
Abnormal	25	9	26	8
Normal	0	29	1	28
<hr/>				

Table 9. Numbers of normal and abnormal Medmont Central Threshold, Humphrey Full Threshold and SITA in the patient sample.

	Medmont Central Threshold (Strict)		Medmont Central Threshold (Loose)	
	Compared with		Compared with	
	Humphreys Full Threshold	Humphreys SITA	Humphreys Full Threshold	Humphreys SITA
Kappa Statistic	0.90	0.87	0.72	0.72
AUC	0.94	0.92		
<u>Sector Correlation (<math>r^2</math> statistic):</u>				
Superonasal	0.86**	0.85**		
Superotemporal	0.80**	0.72**		
Inferonasal	0.69**	0.62**		
Inferotemporal	0.29**	0.23**		
<u>Mean Defect Correlation (<math>r^2</math> statistic):</u>				
	0.89**	0.88**		

(\*P <0.001, \*\*P <0.0001)

Table 10. Comparison of Medmont Central Threshold with Humphreys Full Threshold and Humphreys SITA showing, Kappa Statistic, area under the ROC curve (AUC), quadrant analysis and mean defect correlation.

	Humphrey short wavelength Perimetry		Humphrey frequency doubling perimetry	
	Abnormal	Normal	Abnormal	Normal
<hr/>				
Medmont Flicker (Strict)				
Abnormal	23	8	29	2
Normal	3	29	2	30
<hr/>				
Medmont Flicker (Loose)				
Abnormal	24	10	29	5
Normal	2	27	2	27
<hr/>				

Table 11 Numbers of normal and abnormal Medmont flicker perimetry, Humphrey short wavelength perimetry, and Humphrey frequency doubling perimetry in the patient sample

	Medmont Flicker (Strict)		Medmont Flicker (Loose)	
	Compared with		Compared with	
	Humphreys SWAP	Humphreys FDP	Humphreys SWAP	Humphreys FDP
Kappa Statistic	0.65	0.87	0.62	0.78
AUC	0.81	0.96		
<u>Sector Correlation (<math>r^2</math> statistic):</u>				
Superonasal	0.48**	0.67**		
Superotemporal	0.25**	0.79**		
Inferonasal	0.17*	0.64**		
Inferotemporal	0.02	0.72**		
<u>Mean Defect Correlation (<math>r^2</math> statistic):</u>				
	0.57**	0.79**		

(\*P <0.001, \*\*P <0.0001)

Table 12 Comparison of Medmont flicker perimetry with Humphrey short wavelength perimetry (SWAP) and Humphrey frequency doubling perimetry (FDP) showing kappa statistic, area under the ROC curve (AUC), quadrant analysis, and mean defect correlation

FDP result	SWAP result		
	Abnormal	Normal	Total
All Subjects at Start of Study			
Abnormal	8	2	10
Normal	1	51	52
Total	9	53	62
Subjects With Abnormal AAP Findings at End of Study			
Abnormal	5	0	5
Normal	0	0	0
Total	5	0	5
Subjects With Normal AAP Findings at End of Study			
Abnormal	3	2	5
Normal	1	51	52
Total	4	53	57

Table 13 SWAP Results Compared With FDP Results

---

Global Indices Compared		
Between Tests, $r^2$ (P value)		
Tests Compared	MD	PSD
AAP and SWAP	0.084 (<0.001)	0.122 (<0.001)
AAP and FDP	0.113 (<0.001)	0.021 (0.07)
SWAP and FDP	0.108 (<0.001)	0.005 (0.37)

---

Table 14 Comparison of Global Indices Among AAP, SWAP and FDP Throughout the Study

Quadrant	Univariate Analysis		Multivariate Analysis	
	Coefficient	Test Statistic	Coefficient	Test Statistic
SWAP				
Superonasal	-2.90	10.72****	-2.90	12.09****
Superotemporal	-2.56	9.44****	-2.56	10.90****
Inferonasal	-2.00	6.46****	-2.00	7.62****
Inferotemporal	-1.82	6.79****	-1.82	8.05****
AAP				
Superonasal	-1.57	10.74****	-1.54	11.98****
Superotemporal	-1.70	10.91****	-1.65	12.10****
Inferonasal	-1.54	10.12****	-1.50	11.10****
Inferotemporal	-1.20	7.89****	-1.19	8.57****
FDP				
Superonasal	-0.52	1.32	-0.47	1.14
Superotemporal	-1.16	2.66**	-1.11	2.35*
Inferonasal	-0.80	1.63	-0.70	1.32
Inferotemporal	-1.14	2.63**	-1.05	2.37*

Table 15. Showing Linear Regression Coefficients and Test Statistics for the Relationship between Visual Field Mean Sensitivities and Increasing Eccentricity. Multivariate Analysis was Adjusted for Age.

(Short Wavelength Automated Perimetry: SWAP, Achromatic Automated Perimetry: AAP, Frequency Doubling Perimeter: FDP)

(\* P<0.05, \*\* P<0.01, \*\*\*P<0.001, \*\*\*\*P<0.0001)



FDP		AAP	
		Abnormal	Normal
Conventional Protocol	Abnormal	24	8
	Normal	2	34
Nasal Step	Abnormal	23	5
	Normal	3	37
Arcuate	Abnormal	22	6
	Normal	4	36
Temporal Wedge	Abnormal	16	5
	Normal	10	37

Table 16. Showing Results of Achromatic Automated Perimetry (AAP) Compared with Frequency Doubling Perimetry (FDP) For Each Testing Pattern